Toward extracting scattering phase shifts from integrated correlation functions. V. Complex ϕ^4 field model in 3 + 1 dimensions

Peng Guo[*]

College of Arts and Sciences, Dakota State University, Madison, South Dakota 57042, USA and Kavli Institute for Theoretical Physics, University of California, Santa Barbara, California 93106, USA

Frank X. Lee[†] and Andrei Alexandru[‡]

Physics Department, The George Washington University, Washington, DC 20052, USA

(Received 18 August 2025; accepted 8 October 2025; published 22 October 2025)

In Guo [Toward extracting the scattering phase shift from integrated correlation functions. II. A relativistic lattice field theory model, Phys. Rev. D **110**, 014504 (2024).] and associated studies, a relativistic finite-volume formalism in 1 + 1 dimensions is proposed to extract infinite-volume scattering phaseshift. It is based on the difference of integrated correlation functions rather than energy spectrum in the finite volume, and can be regarded as complementary to the well-known Lüscher formalism. In the present work, the formalism is further extended into 3 + 1 dimensional spacetime. The aim is to explore and demonstrate the challenges in applying the formalism to more practical settings. Specifically, Monte Carlo simulations of a complex ϕ^4 relativistic field model are carried out in both 2 + 1 and 3 + 1 dimensions on lattices of varying sizes, and phaseshifts for the contact interaction are extracted from the formalism using modest computing resources.

DOI: 10.1103/v132-nsb2

I. INTRODUCTION

Scattering is an indispensable tool in studying a wide range of dynamics, from atomic interactions in condensed matter physics to the strong interaction in QCD. Determination of scattering properties in such systems remains fundamental but challenging. In most cases, numerical simulations based on Monte Carlo evaluation of the path integral are performed by placing the system in a finite volume with periodic boundary conditions, which leads to quantized energy spectrum in the system. The energy spectrum is then connected to the infinite volume scattering phaseshifts through quantization conditions.

One such finite-volume formalism known as the Lüscher formula [1] has proven successful in a number of applications, especially in the meson sector, see e.g., Refs. [2–14]. The formalism has also been extended to beyond elastic scattering. see e.g., Refs. [14–44]. However the Lüscher formalism in few-nucleon systems still faces challenges such as the signal-to-noise (S/N) ratio of lattice correlation functions [45,46] and the requirement of increasingly large number of interpolating operators at large volumes [47].

These challenges motivated alternative approaches, such as the potential method of HALQCD Collaboration [48–52], and the integrated correlation functions (ICF) formalism in [53–57]. The latter relates the difference between interacting and noninteracting integrated correlation functions of two particles in a finite volume to the infinite-volume phase shift through a weighted integral. It has the advantage of working directly with correlation functions, bypassing energy spectrum determination in traditional approaches. Additional features include the rapid convergence at short Euclidean times that makes it potentially a good candidate to overcome the S/N problem, and free-by-construction from issues encountered at large volumes, such as increasingly dense energy spectrum and the extraction of low-lying states.

So far, discussions of the integrated correlation functions formalism are mostly limited to 1 + 1 spacetime, including single channel nonrelativistic dynamics [54], relativistic dynamics [53], coupled-channel effect [55], Coulomb corrections [56], and potential implementation on quantum computers [57]. The aim of the present work is to extend it into 3 + 1 spacetime dimensions. We explore and discuss some technical challenges in applying the formalism in

[*]Contact author: peng.guo@dsu.edu
[†]Contact author: fxlee@gwu.edu
[‡]Contact author: aalexan@gwu.edu

Published by the American Physical Society under the terms of the Creative Commons Attribution 4.0 International license. Further distribution of this work must maintain attribution to the author(s) and the published article's title, journal citation, and DOI. Funded by SCOAP[3].

higher dimensions. A relativistic complex ϕ^4 field model on a finite lattice is used as a test bed to demonstrate in detail the feasibility of the integrated correlation functions approach via Monte Carlo simulations. We will show that the formalism converges to the infinite volume limit and phase shifts are accessible in the more practical settings considered here.

The paper is organized as follows. A brief summary of integrated correlation function formalism is outlined in Sec. II, with some technical details given in two appendices. Numerical test by Monte Carlo simulation of a complex ϕ^4 lattice model in both $3+1$ and $2+1$ dimensions is presented in Sec. III, followed by summary in Sec. IV.

II. RELATIVISTIC INTEGRATED CORRELATION FUNCTION FORMALISM IN 3+1 DIMENSIONS

In this section, we outline the extension of relativistic integrated correlation function formalism for complex ϕ^4 theory [53] from $1+1$ to $3+1$ dimensions. More details can be found in Appendix A.

In a periodic cubic box of size L, the correlation function that creates two particles at relative coordinate $\mathbf{r}'$ and time instant 0 and then annihilates them at relative coordinate $\mathbf{r}$ and time instant t is defined by

$$C^{(2\phi)}(\mathbf{r}t;\mathbf{r}'0) = \langle 0|\mathcal{T}[\mathcal{O}(\mathbf{r},t)\mathcal{O}^\dagger(\mathbf{r}',0)]|0\rangle, \tag{1}$$

where $\mathcal{T}$ stands for time-ordered operator. The two-particle creation operator after projecting out center-of-mass motion in the rest frame is given by

$$\mathcal{O}^\dagger(\mathbf{r},t) = \frac{1}{\sqrt{2}}\frac{1}{\sqrt{L^3}}\int_0^L d\mathbf{x}_2 \phi(\mathbf{r}+\mathbf{x}_2,t)\phi(\mathbf{x}_2,t). \tag{2}$$

The factor $1/\sqrt{2}$ takes into account the exchange symmetry of two distinguishable charged particles. The ϕ field satisfies periodic boundary condition; $\phi(\mathbf{x}+L\hat{\mathbf{x}},t) = \phi(\mathbf{x},t)$, where $\hat{\mathbf{x}}$ stands for a unit 3D spatial vector. The correlation function can be decomposed into momentum space and projected into the A_1^+ irreducible representation (irrep) of the cubic symmetry group,

$$C^{(2\phi)}_{A_1^+}(t) = \frac{1}{L^3}\sum_{\mathbf{p}=\frac{2\pi\mathbf{n}}{L},\mathbf{n}\in\mathbb{Z}^3} 2\omega_p \tilde{C}^{(2\phi)}_{A_1^+}(\mathbf{p}t;\mathbf{p}0), \tag{3}$$

where $\omega_p = \sqrt{\mathbf{p}^2+m^2}$, and m is the renormalized mass of ϕ field. The momentum-space components are defined via double Fourier transforms,

$$\tilde{C}^{(2\phi)}(\mathbf{p}t;\mathbf{p}'0) = \int_0^L d\mathbf{r}d\mathbf{r}' e^{i\mathbf{p}\cdot\mathbf{r}} C^{(2\phi)}(\mathbf{r}t;\mathbf{r}'0)e^{-i\mathbf{p}'\cdot\mathbf{r}'}. \tag{4}$$

The A_1^+ irrep projection is defined by double sums over group elements,

$$\tilde{C}^{(2\phi)}_{A_1^+}(\mathbf{p}t;\mathbf{p}'0) = \frac{1}{48^2}\sum_{(g,g')\in\mathcal{G}} \tilde{C}^{(2\phi)}(g\mathbf{p}t;g'\mathbf{p}'0), \tag{5}$$

where $(\mathcal{G},g)$ stand for the octahedral group O_h and its elements, see e.g., Refs. [14,28,58]. The O_h group has 10 irreps ($A_1^\pm$, $A_2^\pm$, $T_1^\pm$, $T_2^\pm$, and $E^\pm$), including parity. The ϕ^4 theory is equivalent to a contact interaction theory, hence only the S-wave contributes to the scattering dynamics, which only requires the A_1^+ irrep.

The integrated correlation function is related to two-particle Green's function on the lattice by

$$C^{(2\phi)}(\mathbf{r}t;\mathbf{r}'0) = i\int_{-\infty}^{\infty}\frac{d\lambda}{2\pi}G^{(L)}(\mathbf{r},\mathbf{r}';\lambda)e^{-i\lambda t}. \tag{6}$$

The two-particle Green's function is the solution of relativistic Dyson equation, with a contact interaction potential,

$$V(\mathbf{r}) = V_0\delta(\mathbf{r}), \tag{7}$$

whose analytic solution is given by

$$G^{(L)}(\mathbf{r},\mathbf{r}';E) - G^{(0,L)}(\mathbf{r}-\mathbf{r}';E) = \frac{G^{(0,L)}(\mathbf{r};E)G^{(0,L)}(\mathbf{r}';E)}{\frac{1}{V_0}-G^{(0,L)}(\mathbf{0};E)}. \tag{8}$$

The noninteracting two-particle Green's function is defined by

$$G^{(0,L)}(\mathbf{r};E) = \frac{1}{L^3}\sum_{\mathbf{q}=\frac{2\pi\mathbf{n}}{L},\mathbf{n}\in\mathbb{Z}^3}\frac{1}{\omega_q}\frac{e^{i\mathbf{q}\cdot\mathbf{r}}}{E^2-(2\omega_q)^2+i0}. \tag{9}$$

The difference of interacting and noninteracting integrated correlation functions is thus given in terms of Green's functions by

$$\begin{aligned}\triangle C^{(2\phi)}_{A_1^+}(t) &= \frac{1}{L^3}\sum_{\mathbf{p}=\frac{2\pi\mathbf{n}}{L},\mathbf{n}\in\mathbb{Z}^3} 2\omega_p[\tilde{C}^{(2\phi)}_{A_1^+}(\mathbf{p}t;\mathbf{p}0) - \tilde{C}^{(0,2\phi)}_{A_1^+}(\mathbf{p}t;\mathbf{p}0)] \\ &= i\int_{-\infty}^{\infty}\frac{d\lambda}{2\pi}e^{-i\lambda t} \times\frac{1}{L^3}\sum_{\mathbf{p}=\frac{2\pi\mathbf{n}}{L},\mathbf{n}\in\mathbb{Z}^3} 2\omega_p[\tilde{G}^{(L)}_{A_1^+}(\mathbf{p},\mathbf{p};\lambda) - \tilde{G}^{(0,L)}_{A_1^+}(\mathbf{0};\lambda)].\end{aligned} \tag{10}$$

The $\tilde{G}^{(L)}_{A_1^+}(\mathbf{p},\mathbf{p};\lambda)$ stands for the irrep projected Green's function in momentum space, which is defined in the same way as in Eq. (5).

Using relativistic Krein's theorem relation in infinite volume (see Appendix A 3),

$$\int_{-\infty}^{\infty}\frac{d\mathbf{p}}{(2\pi)^3}\omega_p[\tilde{G}^{(\infty)}(\mathbf{p},\mathbf{p};E)-\tilde{G}^{(0,\infty)}(\mathbf{0};E)] = -\frac{1}{\pi}\int_{4m^2}^{\infty}ds\frac{\delta(\sqrt{s})}{(s-E^2-i0)^2}, \tag{11}$$

the S-wave scattering phase shift of two scalar particles $\delta(E)$ is connected to the difference of integrated correlation functions in its infinite volume limit through a weighted integral,

$$\triangle C_{A_1^+}^{(2\phi)}(t)\overset{L\to\infty}{\to} -\frac{1}{\pi}\int_{2m}^{\infty}d\epsilon\delta(\epsilon)\frac{d}{d\epsilon}\left(\frac{e^{-i\epsilon t}}{\epsilon}\right). \tag{12}$$

This relation is our main result (we will refer to it as the *ICF formula* for short). Its Euclidean spacetime version can be written in the form,

$$\triangle C_{A_1^+}^{(2\phi)}(\tau)\overset{L\to\infty}{\to}\frac{1}{\pi}\int_{2m}^{\infty}d\epsilon\delta(\epsilon)\left(\tau+\frac{1}{\epsilon}\right)\frac{e^{-\epsilon\tau}}{\epsilon} \tag{13}$$

after analytic continuation ($t\to -i\tau$) and derivative. This relation will be verified via Monte Carlo simulation in the next section. We should mention that although the above two formulas are presented in the context of a ϕ^4 theory and contact interactions, they are more generally applicable to other field theory models, such as lattice QCD. If projection to other irreps is required, a partial-wave expansion of the relations can be utilized, see Appendix A.

III. MONTE CARLO SIMULATION TEST

We consider the complex ϕ^4 action on a $3+1$ Euclidean spacetime lattice, see e.g., Refs. [32,53],

$$S_E = -\kappa\sum_{\mathbf{x},\tau,\hat{\mathbf{n}}_\mathbf{x},\hat{n}_\tau}\hat{\phi}^*(\mathbf{x},\tau)\hat{\phi}(\mathbf{x}+\hat{\mathbf{n}}_\mathbf{x},\tau+\hat{n}_\tau)+\text{c.c.} + (1-2\lambda)\sum_{\mathbf{x},\tau}|\hat{\phi}(\mathbf{x},\tau)|^2+\lambda\sum_{\mathbf{x},\tau}|\hat{\phi}(\mathbf{x},\tau)|^4, \tag{14}$$

where $(\mathbf{x},\tau)$ label the discrete coordinates of Euclidean $L^3\times T$ lattice sites: $(x,y,z)\in[0,L-1]$ and $\tau\in[0,T-1]$, and $(\hat{\mathbf{n}}_\mathbf{x},\hat{n}_\tau)$ denote the unit vectors in direction $(\mathbf{x},\tau)$. The ϕ field is rescaled on the lattice,

$$\phi(\mathbf{x},\tau)=\sqrt{2\kappa}\hat{\phi}(\mathbf{x},\tau), \tag{15}$$

and it satisfies periodic boundary conditions in all directions. The parameters (κ,λ) are related to bare mass m_0 and bare coupling constant g_0 of interacting term $\frac{g_0}{4!}|\phi|^4$ by

$$m_0^2=\frac{1-2\lambda}{\kappa}-8 \quad\text{and}\quad g_0=\frac{6\lambda}{\kappa^2}. \tag{16}$$

The lattice spacing a is absorbed by rescaling in the parameters. If needed, the a dependence can be restored by lattice units, $L\to L/a$, $m\to am$, etc. The ϕ^4 term describes a contact interaction in the theory. The bare interaction strength V_0 in the contact potential model in Eq. (7) can be adjusted by tuning λ.

Monte Carlo (MC) simulation is carried out by the hybrid Monte Carlo (HMC) algorithm, see details in Ref. [32]. The single particle and two-particle correlation functions are evaluated respectively by path integrals,

$$C_{\text{lat}}^{(\phi)}(\mathbf{x}\tau,\mathbf{x}'0)=\frac{\int\mathcal{D}\phi\mathcal{D}\phi^\dagger\phi^\dagger(\mathbf{x},\tau)\phi(\mathbf{x}',0)e^{-S_E}}{\int\mathcal{D}\phi\mathcal{D}\phi^\dagger e^{-S_E}} \tag{17}$$

and

$$C_{\text{lat}}^{(2\phi)}(\mathbf{r}\tau,\mathbf{r}'0)=\frac{\int\mathcal{D}\phi\mathcal{D}\phi^\dagger\mathcal{O}(\mathbf{r},\tau)\mathcal{O}^\dagger(\mathbf{r}',0)e^{-S_E}}{\int\mathcal{D}\phi\mathcal{D}\phi^\dagger e^{-S_E}}, \tag{18}$$

where subscript-lat is added to denote the Monte Carlo simulation result, and the relative motion of two-particle interpolating operator is defined in Eq. (B4).

On the lattice, the *integrated* single-particle correlation function is defined by discrete sums over coordinates,

$$C_{\text{lat}}^{(\phi)}(\tau)=\sum_{\mathbf{x}\in[0,L-1]^3}C_{\text{lat}}^{(\phi)}(\mathbf{x}\tau,\mathbf{x}0), \tag{19}$$

and the *integrated* A_1^+-projected two-particle correlation function is defined by discrete sums over momentum,

$$C_{A_1^+,\text{lat}}^{(2\phi)}(\tau)=\frac{1}{L^3}\sum_{\mathbf{p}=\frac{2\pi\mathbf{n}}{L}}^{\mathbf{n}\in[-\frac{L}{2}+1,\frac{L}{2}]^3}2\omega_\mathbf{p}^{(\text{lat})}\tilde{C}_{A_1^+,\text{lat}}^{(2\phi)}(\mathbf{p}\tau,\mathbf{p}0), \tag{20}$$

where the lattice dispersion relation is given by

$$\omega_\mathbf{p}^{(\text{lat})}=\cosh^{-1}\left[3+\cosh m-\sum_{i=x,y,z}\cos\mathbf{p}_i\right]. \tag{21}$$

The Fourier transform of one or two particles correlation functions is defined by

$$\tilde{C}_{\text{lat}}^{(\phi,2\phi)}(\mathbf{p}\tau,\mathbf{p}'0)=\sum_{\mathbf{x},\mathbf{x}'\in[0,L-1]^3}e^{i\mathbf{p}\cdot\mathbf{x}}C_{\text{lat}}^{(\phi,2\phi)}(\mathbf{x}\tau,\mathbf{x}'0)e^{-i\mathbf{p}'\cdot\mathbf{x}'}, \tag{22}$$

where the discrete momenta in the three spatial dimensions are indicated by

$$(\mathbf{p},\mathbf{p}')=\frac{2\pi\mathbf{n}}{L},\qquad \mathbf{n}\in\left[-\frac{L}{2}+1,\frac{L}{2}\right]^3. \tag{23}$$

The most challenging part is to compute the integrated two-particle correlation functions in Eq. (20) which involves multiple nested 3D sums. We show in the

following that this challenge can be overcome by Fourier transform. If the ϕ field is transformed as

$$\tilde{\phi}(\mathbf{p},\tau) = \sum_{\mathbf{x}\in[0,L-1]^3} e^{i\mathbf{p}\cdot\mathbf{x}}\phi(\mathbf{x},\tau), \tag{24}$$

then Eq. (20) can be expressed in momentum space as

$$C^{(2\phi)}_{A_1^+,\mathrm{lat}}(\tau) = \frac{1}{L^3}\sum_{\mathbf{p}=\frac{2\pi\mathbf{n}}{L}}^{\mathbf{n}\in[-\frac{L}{2}+1,\frac{L}{2}]^3} 2\omega^{(\mathrm{lat})}_{\mathbf{p}}\langle 0|\tilde{\mathcal{O}}_{A_1^+}(\mathbf{p},\tau)\tilde{\mathcal{O}}^{\dagger}_{A_1^+}(\mathbf{p},0)|0\rangle. \tag{25}$$

The irrep-projected two-particle correlation function is defined by

$$\tilde{\mathcal{O}}^{\dagger}_{A_1^+}(\mathbf{p},\tau) = \frac{1}{48}\sum_{g\in\mathcal{G}}\tilde{\mathcal{O}}^{\dagger}(g\mathbf{p},\tau), \tag{26}$$

where

$$\tilde{\mathcal{O}}^{\dagger}(\mathbf{p},\tau) = \frac{1}{\sqrt{2}}\frac{1}{\sqrt{L^3}}\tilde{\phi}(\mathbf{p},\tau)\tilde{\phi}(-\mathbf{p},\tau). \tag{27}$$

Using the identity,

$$\sum_{\mathbf{p}=\frac{2\pi\mathbf{n}}{L}}^{\mathbf{n}\in[-\frac{L}{2}+1,\frac{L}{2}]^3} = \sum_{\mathbf{p}_0=\frac{2\pi\mathbf{n}}{L}}^{\mathbf{n}\in[0,\frac{L}{2}]^3}\frac{\vartheta(\mathbf{p}_0)}{\sigma_{\mathbf{p}_x}\sigma_{\mathbf{p}_y}\sigma_{\mathbf{p}_z}}, \tag{28}$$

where the symmetry factor $\sigma_{\mathbf{p}_i}$ is defined by

$$\sigma_{\mathbf{p}_i} = \begin{cases} 2, & \text{if } \frac{L}{2\pi}\mathbf{p}_i = \frac{1}{2}, \\ 1, & \text{otherwise,} \end{cases} \tag{29}$$

Eq. (25) can be further reduced to

$$C^{(2\phi)}_{A_1^+,\mathrm{lat}}(\tau) = \frac{1}{L^3}\sum_{\mathbf{p}_0=\frac{2\pi\mathbf{n}_0}{L}}^{\mathbf{n}_0\in[0,\frac{L}{2}]^3}\frac{\vartheta(\mathbf{p}_0)}{\sigma_{\mathbf{p}_x}\sigma_{\mathbf{p}_y}\sigma_{\mathbf{p}_z}} \times 2\omega^{(\mathrm{lat})}_{\mathbf{p}_0}\langle 0|\tilde{\mathcal{O}}_{A_1^+}(\mathbf{p}_0,\tau)\tilde{\mathcal{O}}^{\dagger}_{A_1^+}(\mathbf{p}_0,0)|0\rangle. \tag{30}$$

The $\mathbf{p}_0$ denote a single reference vector in cubic symmetry group. It is the set of momenta represented by $\mathbf{p}_0$ via $\mathbf{p} = g\mathbf{p}_0 (g\in\mathcal{G})$. The $\vartheta(\mathbf{p}_0)$ is the multiplicity of distinct momenta within the set represented by $\mathbf{p}_0$, see e.g., Refs. [14,28,58] and also see some details in Appendix B.

In summary, computation of the two-particle integrated correlation function can be greatly accelerated by employing Fourier transform of the ϕ field. We precompute the transform by using a Fast Fourier Transform software package called *fftw3* and store it in memory. As a result, the cost of computing integrated two-particle correlation function is on par with that of single-particle ones.

A. Exact solutions for noninteracting case: $\lambda = 0$

In the absence of interactions, i.e., setting $\lambda = 0$ in Euclidean action in Eq. (14), analytic expressions of correlation functions can be obtained, see e.g., Ref. [53]. This fact can be used to numerically check some basic properties of the Monte Carlo simulation. First, single-particle correlation in $3+1$ dimensions is given by

$$C^{(0,\phi)}(\mathbf{x}\tau,\mathbf{x}'0) = \frac{1}{L^3}\sum_{\mathbf{k}=\frac{2\pi\mathbf{n}}{L}}^{\mathbf{n}\in[-\frac{L}{2}+1,\frac{L}{2}]^3} e^{i\mathbf{k}\cdot(\mathbf{x}-\mathbf{x}')}G_{\phi}(\mathbf{k},\tau), \tag{31}$$

and two-particle correlation function by

$$C^{(0,2\phi)}(\mathbf{r}\tau,\mathbf{r}'0) = \frac{1}{L^3}\sum_{\mathbf{k}=\frac{2\pi\mathbf{n}}{L}}^{\mathbf{n}\in[-\frac{L}{2}+1,\frac{L}{2}]^3}\cos(\mathbf{k}\cdot\mathbf{r})\cos(\mathbf{k}\cdot\mathbf{r}') \times [G_{\phi}(\mathbf{k},\tau)]^2. \tag{32}$$

The Green's function in the above expressions is defined by

$$G_{\phi}(\mathbf{k},\tau) = \frac{1}{T}\sum_{\omega=\frac{2\pi n}{T}}^{n\in[0,T-1]}\frac{e^{i\omega\tau}}{\sum_{i=x,y,z}(2-2\cos\mathbf{k}_i)-2\cos\omega+2\cosh m}. \tag{33}$$

Next, using the Fourier transform in Eq. (22), the integrated one-particle correlation function is reduced to a single sum on the Green's function,

$$C^{(0,\phi)}(\tau) = \frac{1}{L^3}\sum_{\mathbf{p}=\frac{2\pi\mathbf{n}}{L}}^{\mathbf{n}\in[-\frac{L}{2}+1,\frac{L}{2}]^3}\tilde{C}^{(0,\phi)}(\mathbf{p}\tau,\mathbf{p}0) = \sum_{\mathbf{p}=\frac{2\pi\mathbf{n}}{L}}^{\mathbf{n}\in[-\frac{L}{2}+1,\frac{L}{2}]^3} G_{\phi}(\mathbf{p},\tau). \tag{34}$$

The integrated two-particle correlation function is reduced to double sums over momenta,

$$C^{(0,2\phi)}_{A_1^+}(\tau) = \frac{1}{L^3}\sum_{\mathbf{p}=\frac{2\pi\mathbf{n}}{L}}^{\mathbf{n}\in[-\frac{L}{2}+1,\frac{L}{2}]^3} 2\omega^{(\mathrm{lat})}_{\mathbf{p}}\tilde{C}^{(0,2\phi)}_{A_1^+}(\mathbf{p}\tau,\mathbf{p}0) = \sum_{(\mathbf{p},\mathbf{k})\in\frac{2\pi\mathbf{n}}{L}}^{\mathbf{n}\in[-\frac{L}{2}+1,\frac{L}{2}]^3} 2\omega^{(\mathrm{lat})}_{\mathbf{p}}\sigma^{(\mathrm{lat})}_{\mathbf{p},\mathbf{k}}[G_{\phi}(\mathbf{k},\tau)]^2, \tag{35}$$

where the weighting factor is defined by

$$\sigma^{(\mathrm{lat})}_{\mathbf{p},\mathbf{k}} = \left| \frac{1}{48} \sum_g \frac{1}{L^3} \int d\mathbf{r} e^{ig\mathbf{p}\cdot\mathbf{r}} \cos(\mathbf{k}\cdot\mathbf{r}) \right|^2 = \begin{cases} \frac{\sigma^2_{\mathbf{p}_x}\sigma^2_{\mathbf{p}_y}\sigma^2_{\mathbf{p}_z}}{\vartheta^2(\mathbf{p}_0)}, & \text{if } (\mathbf{k},\mathbf{p}) \in g\mathbf{p}_0, \text{where } g \in \mathcal{G}, \\ 0, & \text{otherwise.} \end{cases} \tag{36}$$

Using the identity in Eq. (28) again, Eq. (35) can be further reduced to a single sum,

$$C^{(0,2\phi)}_{A_1^+}(\tau) = \sum_{\mathbf{p}_0 = \frac{2\pi\mathbf{n}_0}{L}}^{\mathbf{n}_0 \in [0,\frac{L}{2}]} 2\omega^{(\mathrm{lat})}_{\mathbf{p}_0} [G_\phi(\mathbf{p}_0,\tau)]^2. \tag{37}$$

In the continuum limit of $a \to 0$ and $T \to \infty$, the integrated correlation functions approach known forms for free particles,

$$C^{(0,\phi)}(\tau) \underset{a\to 0}{\overset{T\to\infty}{\to}} \sum_{\mathbf{p}=\frac{2\pi\mathbf{n}}{L}}^{\mathbf{n}\in\mathbb{Z}^3} \frac{e^{-\omega_p \tau}}{2\omega_p}, \tag{38}$$

and

$$C^{(0,2\phi)}_{A_1^+}(\tau) \underset{a\to 0}{\overset{T\to\infty}{\to}} \sum_{\mathbf{p}_0} \frac{e^{-2\omega_{p_0}\tau}}{2\omega_{p_0}}, \tag{39}$$

where $\omega_q = \sqrt{\mathbf{q}^2 + m^2}$ for both $\mathbf{q} = \mathbf{p}$ and $\mathbf{q} = \mathbf{p}_0$. It serves as another consistency check of the formalism.

Monte Carlo simulations are performed for noninteracting charged scalar particles with the following choice of parameters; $\kappa = 0.0618$, and $\lambda = 0$, fixed temporal extent $T = 60$, spatial extent $L = 10$, and 200k configurations. The mass of the single particle is measured by fitting single-particle correlation function $\tilde{C}^{(0,\phi)}(\mathbf{p}\tau, \mathbf{p}0)$ at zero momentum ($\mathbf{p} = 0$). We find $m = 0.299 \pm 0.004$. Note that m is the only free parameter in the single-particle correlation function which appears via Eq. (33).

The effective mass defined by

$$m^{(\phi,2\phi)}_{\mathrm{eff}}(\mathbf{p},\tau) = \ln \frac{\tilde{C}^{(\phi,2\phi)}_{\mathrm{lat}}(\mathbf{p}\tau,\mathbf{p}0)}{\tilde{C}^{(\phi,2\phi)}_{\mathrm{lat}}(\mathbf{p}(\tau+1),\mathbf{p}0)}, \tag{40}$$

is plotted in Fig. 1 for free single-particle correlation functions at different momenta. The signal is good at zero momentum, but deteriorates increasingly at nonzero momenta.

The lattice dispersion relation in Eq. (21) is checked in Fig. 2 using lattice momentum,

$$p^2 = 4 \sum_{i=x,y,z} \sin^2\left(\frac{\mathbf{p}_i}{2}\right), \tag{41}$$

and the measured mass and energies in Fig. 1. We see that the relation is well-satisfied, albeit with larger errors at higher momenta.

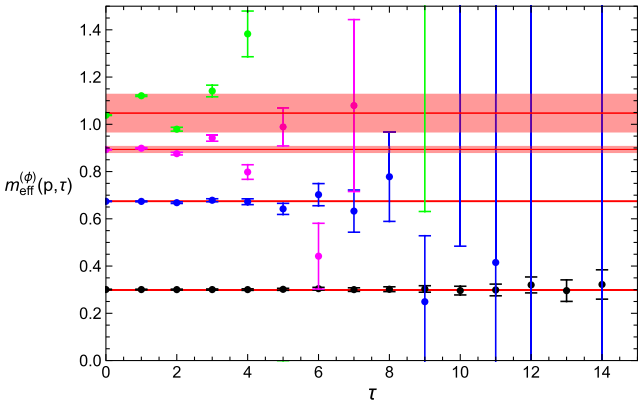


FIG. 1. Noninteracting single-particle effective mass from Monte Carlo data of $m^{(\phi)}_{\mathrm{eff}}$ in Eq. (40) at the lowest three momenta $\mathbf{p} = 2\pi\mathbf{n}/L$ with $\mathbf{n} = (0,0,0)$ (black), (1, 0, 0) (blue), (1, 1, 0) (purple), and (1, 1, 1) (green). The fit results (red bands) are also indicated.

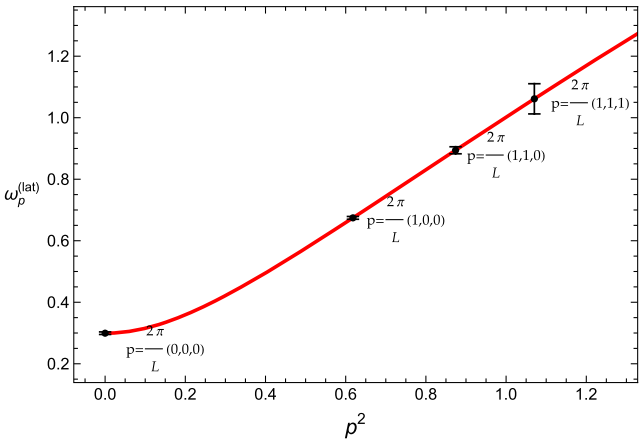


FIG. 2. Lattice dispersion relation defined in Eq. (21) is compared with the simulation results measured in Fig. 1.

Next, in Fig. 3 we check the lattice results against the exact single-particle integrated correlation function in Eq. (34) by plotting $1 - C^{(0,\phi)}(\tau)/C^{(\phi)}_{\mathrm{lat}}(\tau)$ which should approach zero for perfect agreement. We see good agreement at small times. The noninteracting two-particle integrated function is checked in Fig. 4 against Eq. (35). Similar agreement is observed at small times, but worse signal at large times. The two-particle correlation function takes as input the mass m fitted from the single-particle correlation function.

B. Phase shift analysis in interacting cases: $\lambda \neq 0$

Monte Carlo simulations for interacting charged scalar particles are carried out with the following choice of parameters; $\kappa = 0.0666$, and $\lambda = 0.03$, $T = 60$, and spatial extents ranging from $L = 4$ to 28. We use statistics on the order of 200k measurements for each case.

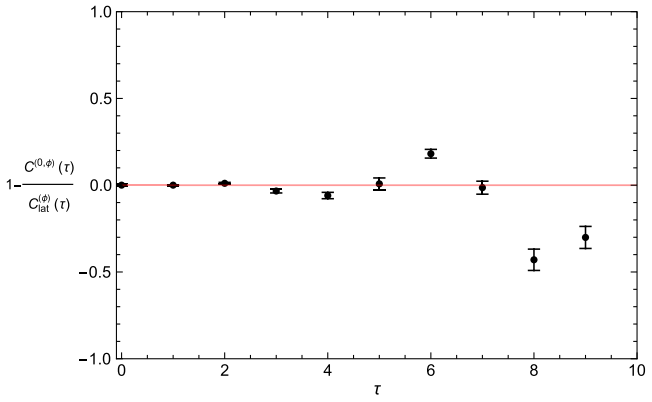


FIG. 3. Comparison of lattice results for noninteracting single-particle integrated correlation function against the exact expression in Eq. (34). The parameters are $T = 60$, $L = 10$, $\kappa = 0.0618$, and $\lambda = 0$.

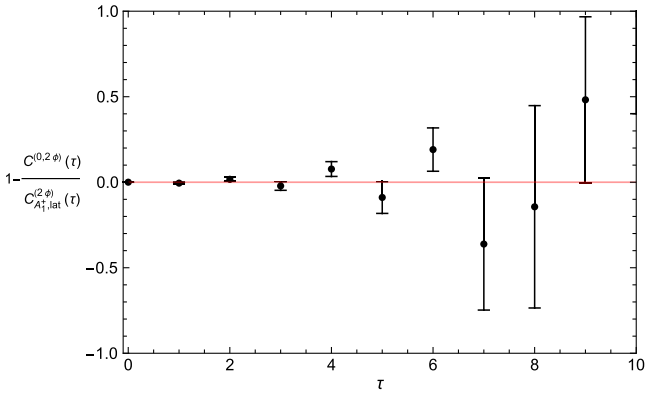


FIG. 4. Similar to Fig. 3, but for the free two-particle integrated correlation function in Eq. (35).

The single-particle mass is measured by fitting momentum-projected single-particle correlation function $\tilde{C}^{(0,\phi)}(\mathbf{p}\tau, \mathbf{p}0)$ with $\mathbf{p} = 0$. Figure 5 shows an example of single-particle effective mass at several momenta. The data quality is fairly good at all momenta considered. Interestingly, the interacting signal is better than that in the noninteracting case in Fig. 1.

In Fig. 6 we fit our data to the well-known lattice size dependence of single-particle mass, see e.g., Ref. [15],

$$m(L) = m + \frac{c}{\sqrt{L^3}} e^{-mL}, \tag{42}$$

and obtain $m = 0.17084 \pm 0.0003$ and $c = 1.92 \pm 0.02$. It is smaller than the one ($m = 0.299$) in the noninteracting case. This mass in the interacting case is used as input in two-particle correlation functions.

Figure 7 shows the comparison plot of single-particle integrated correlation function $1 - C^{(0,\phi)}(\tau)/C^{(\phi)}_{\rm lat}(\tau)$. This figure differs from Fig. 3 mainly in that one is interacting

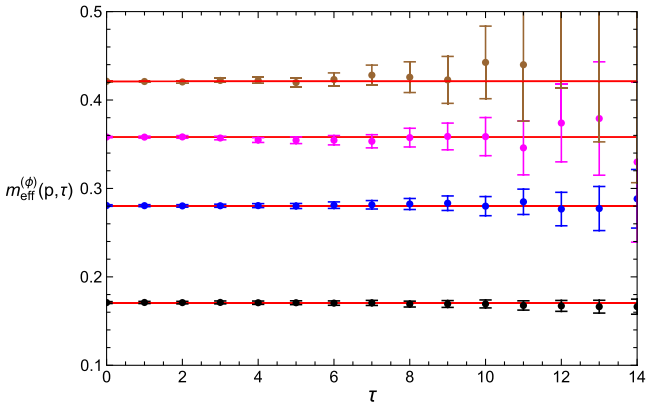


FIG. 5. Interacting single-particle effective mass plot: Monte Carlo data (colored points with error bars) vs. fit results (red bands). The color coding for momentum $\mathbf{p} = \frac{2\pi}{L}\mathbf{n}$ with $\mathbf{n} = (0,0,0)$ (black), (1, 0, 0) (blue), (1, 1, 0) (purple), and (1, 1, 1) (brown). The parameters are: $T = 60$, $L = 28$, $\kappa = 0.0666$, and $\lambda = 0.03$.

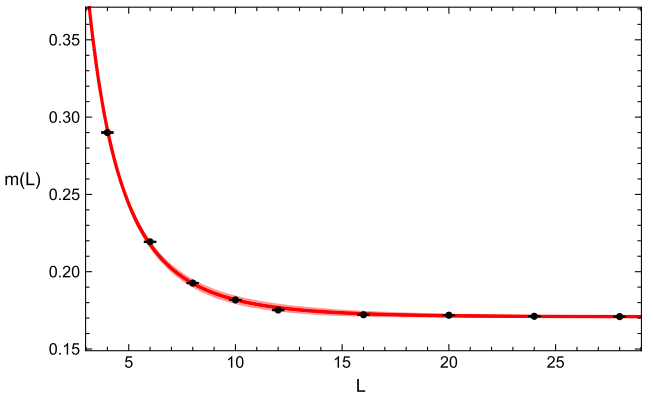


FIG. 6. Lattice size dependence of interacting single-particle mass in Eq. (42) is fitted to MC data using the parameters $T = 60$, $\kappa = 0.06255$ and $\lambda = 0.005$.

case ($\kappa = 0.0666$, $\lambda = 0.03$, and $m = 0.17084$), and the other noninteracting ($\kappa = 0.0618$, $\lambda = 0$, and $m = 0.299$).

To verify the main relation in Eq. (13), first, the difference of integrated two-particle correlation functions between lattice MC data and noninteracting analytic expression (left-hand side),

$$\triangle C^{(2\phi)}_{A_1^+}(\tau) = C^{(2\phi)}_{A_1^+,\rm lat}(\tau) - C^{(0,2\phi)}_{A_1^+}(\tau), \tag{43}$$

is computed on various lattices of size $L = 12$, 16, 20, 24, and 28. Here the interacting term is given in Eq. (20), and the noninteracting term in Eq. (35). Next, we employ perturbation result for the right-hand side,

$$\triangle C^{(2\phi)}_{\rm pert}(\tau) = -\frac{V_R(0)}{L^3} \sum_{\mathbf{p}=\frac{2\pi\mathbf{n}}{L}}^{\mathbf{n}\in\mathbb{Z}^3} \frac{\tau + \frac{1}{2\omega_\mathbf{p}}}{(2\omega_\mathbf{p})^3} e^{-2\omega_\mathbf{p}\tau}, \tag{44}$$

to fit the difference on the left-hand side to obtain the renormalized coupling strength $V_R(0)$ in the contact interaction. The perturbation expression is L dependent. Details of the perturbation expansion are outlined in Appendix B 4.

Once the renormalized coupling strength $V_R(0)$ is extracted, the S-wave phase shift can be obtained by the quantization condition, see Appendix A,

$$\delta(E) = \cot^{-1}\left[-\frac{\frac{1}{V_R(0)} - \mathrm{Re}[G(E)] + G(0)}{\rho(E)}\right], \quad (45)$$

where

$$G(E) = \frac{\rho(E)}{\pi}\ln\frac{\rho(E)+1}{\rho(E)-1}, \quad (46)$$

and

$$\rho(E) = \frac{1}{16\pi}\sqrt{1-\frac{4m^2}{E^2}}. \quad (47)$$

Finally, the result is compared with the infinite volume limit on the right-hand side of Eq. (13) with input from $V_R(0)$ determined in perturbation theory and phase shift expression in Eq. (45).

The result from the above-mentioned analysis strategy is summarized in Fig. 8. Although the complex ϕ^4 theory is a relatively simple field model, its MC simulation in $3+1$ dimensions is still a demanding numerical undertaking, especially on large lattices. With configurations on the order of 200k, the overall quality of the signal in Fig. 8 is not ideal. Specifically, the $L = 28$ signal for $\triangle C^{(2\phi)}_{A_1^+}(\tau)$

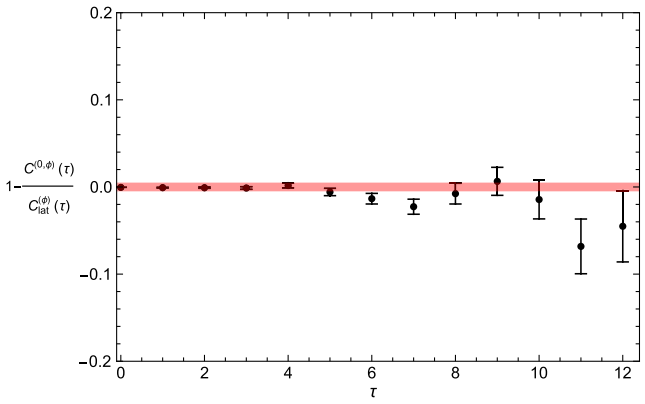


FIG. 7. Comparison of lattice vs. exact single-particle integrated correlation functions for the interacting case in $3+1$ dimensions. The parameters are $T = 60$, $L = 28$, $\kappa = 0.0666$, and $\lambda = 0.03$.

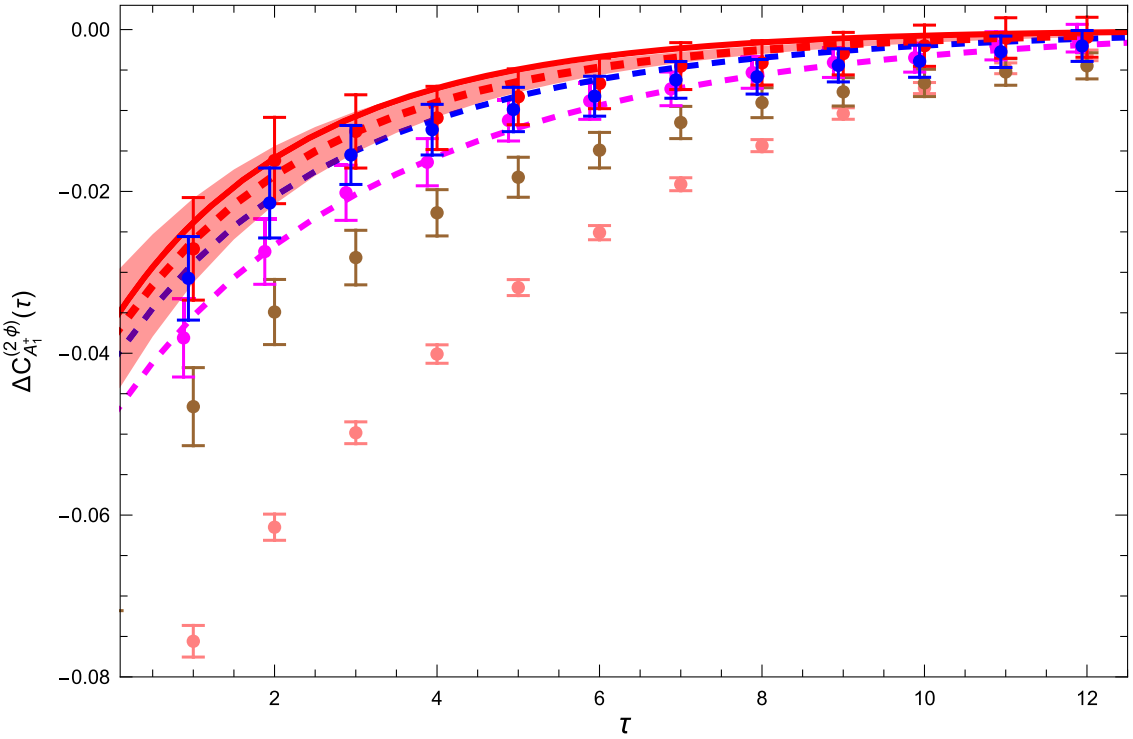


FIG. 8. Convergence of the relation in Eq. (13) in $3+1$ dimensions. The left-hand side $\triangle C^{(2\phi)}_{A_1^+}(\tau)$ from MC simulation is shown as data points on lattices of size $L = 12$ (pink), 16 (brown), 20 (magenta), 24 (blue) and 28 (red). The data points for $L = 20, 24$ are slightly shifted horizontally for better viewing. The perturbation result is color-matched for $L = 20$ (dashed magenta), 24 (dashed blue), and 28 (dashed red). The red band is uncertainty propagated from fitting $L = 24, 28$ to perturbation result to obtain V_R. The infinite volume limit is the solid red curve. The fixed parameters are $T = 60$, $\kappa = 0.0666$, and $\lambda = 0.03$.

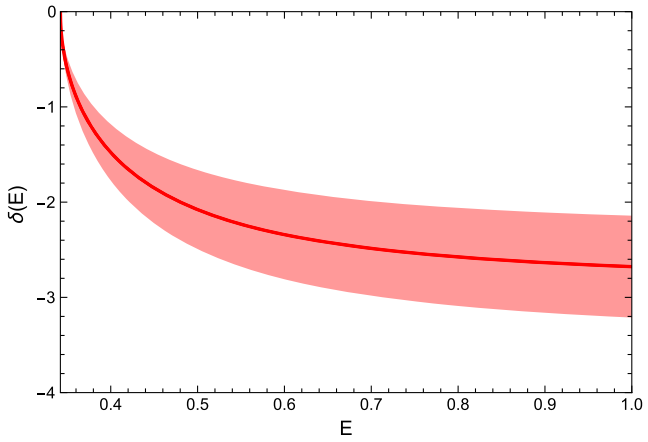


FIG. 9. Phase shift (in degrees) as a function of energy extracted from Eq. (45) in $3+1$ dimensions.

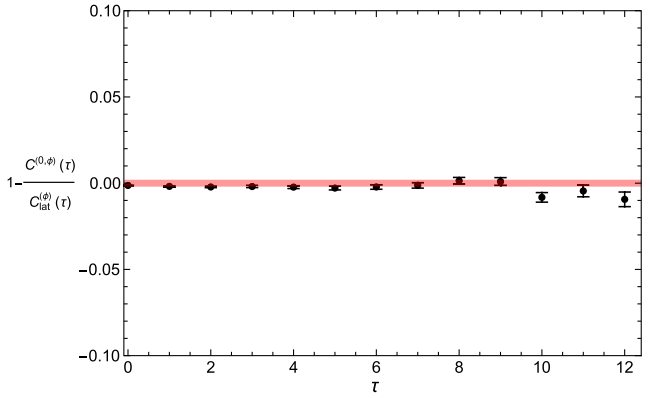


FIG. 10. Comparison of lattice vs. exact single-particle integrated correlation functions in $2+1$ dimensions. The parameters are: $T=60$, $L=28$, $\kappa=0.0875$, and $\lambda=0.02$. Its counterpart in $3+1$ dimensions is Fig. 7.

fluctuates for $\tau>4$, which is also observed in the single-particle correlation function in Fig. 7. Nonetheless, the convergence of the relation to the infinite volume limit is clearly visible as L is increased, despite the relatively large uncertainties in the data at $L=24$, 28. Fitting the signal from these two lattices with perturbation theory, we can get a estimate of the renormalized contact interaction potential strength, $V_R(0)=2.5\pm0.5$. Using this value, the phase shift can be extracted via Eq. (45), as illustrated in Fig. 9. The uncertainty band is a direct consequence of the large uncertainties in the two-particle ICF signal. As the signal improves, the band is expected to shrink accordingly, as confirmed next.

C. Sanity check in 2+1 dimensions

To lend support for the extension from $1+1$ to $3+1$ dimensions, we consider the in-between case of $2+1$ dimensions in this section. The reduction of the formalism from $3+1$ dimensions presented in previous sections down to $2+1$ dimensions is fairly straightforward. The main relation in Eq. (13) takes the same form. All the definitions of one- and two-particle correlation functions remain the same. The primary difference lies in the expression of S-wave phase shift, and symmetry group projections in $2+1$ dimensions.

The scattering amplitude and S-wave phase shift for the complex ϕ^4 theory in $2+1$ dimensions can be derived in a similar way to $3+1$, as detailed in the appendixes. Here we only point the crucial differences for the convergence test. The free particle Green's function at origin is now given by

$$G^{(0,\infty)}(\mathbf{0};E)=\frac{1}{8\pi}\int_{4m^2}^{\infty}\frac{ds'}{s'}\frac{\sqrt{s'}}{E^2-s'+i0}, \tag{48}$$

whose analytic expression is free of ultraviolet divergence,

$$G^{(0,\infty)}(\mathbf{0};E)=G(E)=\frac{1}{8\pi E}\ln\frac{\frac{2m}{E}-1}{\frac{2m}{E}+1}. \tag{49}$$

Hence the coupling strength of the contact interaction in $2+1$ dimensions does not require renormalization. The scattering amplitude is given simply by

$$t(E)=-\frac{1}{\frac{1}{V_0}-G(E)}=\frac{1}{\rho(E)}\frac{1}{\cot\delta(E)-i}, \tag{50}$$

where the phase space factor is defined by

$$\rho(E)=\frac{1}{8E}. \tag{51}$$

The analytic expression of S-wave phase shift is related to V_0 by

$$\delta(E)=\cot^{-1}\left[\frac{\frac{1}{V_0}-\mathrm{Re}[G(E)]}{\mathrm{Im}\,[G(E)]}\right]. \tag{52}$$

The symmetry group is reduced from that of a cube (octahedral group O_h with 48 elements) in $3+1$ dimensions to that of a square (dihedral group D_4 with 8 elements) in $2+1$ dimensions. The D_4 group has five irreps (A_1, A_2, B_1, B_2, and E), not counting parity. The projection to the A_1 irrep corresponds to the S-wave in $2+1$ dimensions,

$$\tilde{C}^{(2\phi)}_{A_1}(\mathbf{p}t;\mathbf{p}'0)=\frac{1}{8^2}\sum_{(g,g')\in\mathcal{G}}\tilde{C}^{(2\phi)}(g\mathbf{p}t;g'\mathbf{p}'0), \tag{53}$$

where the $(\mathcal{G},g)$ now refer to the D_4 group and its elements.

The computational demand in $2+1$ dimensions scales down by about a factor of L relative to $3+1$ dimensions. Consequently, we can perform high-statistics Monte Carlo

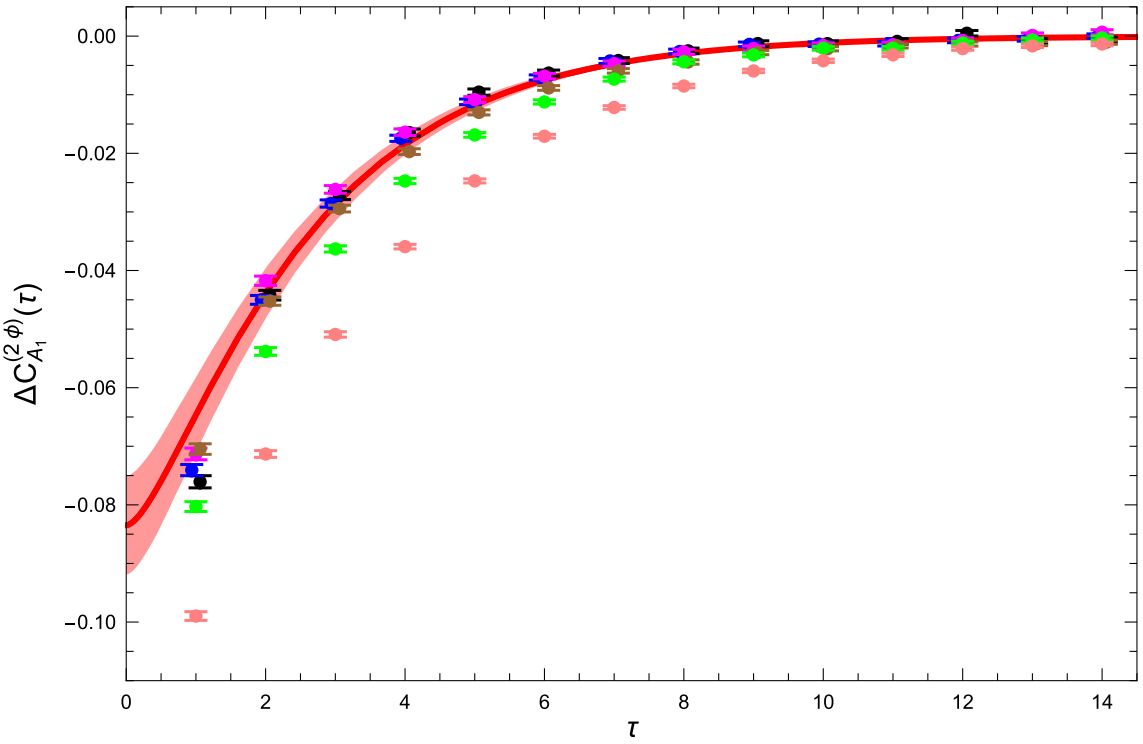


FIG. 11. Convergence of the relation in Eq. (13) in $2+1$ dimensions. The left-hand side $\triangle C_{A_1}^{(2\phi)}(\tau)$ from MC simulation is shown as data points on lattices of size $L = 12$ (pink), 16 (green), 20 (brown), 24 (blue), 28 (magenta), and 32 (black). The infinite volume limit is the solid red curve. Other parameters are $T = 60$, $\kappa = 0.0875$, and $\lambda = 0.02$.

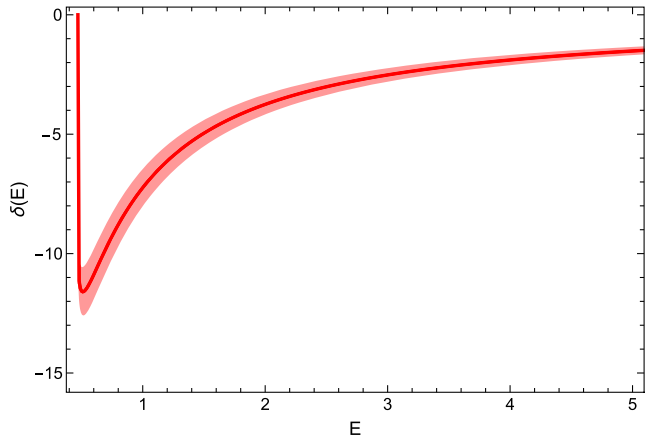


FIG. 12. Phase shift (in degrees) extracted from Eq. (52) in $2+1$ dimensions.

simulations, typically a million configurations for each case. For interacting charged scalar particles we use the following parameters; $\kappa = 0.0875$, and $\lambda = 0.02$. The temporal extent of the lattice is again fixed at $T = 60$, and multiple lattices up to $L = 32$ are considered. The single-particle mass is found with relatively high precision; $m = 0.2353 \pm 0.0003$. The single-particle integrated correlation function from MC simulation matches well with the exact result up to $\tau = 9$, as shown in Fig. 10. The convergence test is given in Fig. 11 for $L = 12$, 16, 20, 24, 28, 32. We see that, with high statistics, the finite-volume lattice results for $L = 24$, 28, 32 demonstrate excellent convergence and match the infinite volume result fairly well overall. Small deviations are observed at time $\tau = 1$ between the lattice data and its infinite volume limit. The cause of the deviation is not clear at the moment. It could be an indication of inelastic contribution or the noisy signal of Monte Carlo simulation at high energies. Nonetheless, we obtain $V_0 = 1.1 \pm 0.1$ for the coupling strength in the contact interaction potential directly by fitting the right-hand side of Eq. (13) using data on $L = 24$, 28, 32, and Eq. (52). The phase shift extracted from the same fit using Eq. (52) is illustrated in Fig. 12, which has a much smaller uncertainty band compared to that in Fig. 9 for $3+1$ dimensions.

IV. SUMMARY AND CONCLUSION

In this work, we extend the relativistic ICF formalism developed in Refs. [53–57] to higher dimensions. The central result is the ICF formula in Eqs. (12) or (13) that relates the difference of interacting and noninteracting integrated correlation functions in finite volume to scattering phase shifts in infinite volume through a weighted integral. It can be regarded as a complementary method to the well-known Lüscher formalism. The extension is an

important step in applying the formalism toward more realistic applications.

Specifically, we carry out Monte Carlo simulations of a complex ϕ^4 field theory model on $L^3 \times T$ lattices in $3+1$ dimensions. Such a model simulates a relativistic scalar field interacting with a contact interaction potential. The main result is summarized in Fig. 8 obtained on lattices up to $L = 28$ and statistics on the order of 200k. Despite the simplicity of the model, a decent amount of computational resources is needed for the numerical demonstration. The convergence to the infinite volume limit is clearly visible but not ideal on large lattices. Nonetheless, the lattice data can be fitted against perturbation theory to extract the strength of contact interaction potential from which the scattering phase shift is determined.

Moreover, the features observed in $3+1$ dimensions are buttressed by a companion simulation in $2+1$ dimensions where the computational burden is much alleviated and high statistics can be employed. The corresponding result in Fig. 11 confirms the general conclusion in $3+1$ dimensions but the signal is much cleaner, and the phase shift can be extracted with a much smaller uncertainty.

These results inspire confidence that extracting phase shift in finite volume from the ICF approach is practical for quantum field theories in $3+1$ dimensions. Reflecting on the experience, the accurate modeling of noninteracting two-particle correlation function in Eq. (13) is a key ingredient for success. In ϕ^4 theory, the noninteracting two-particle correlation function in Eq. (37) is an analytic function that depends only on the effective mass of the single particle; no other renormalization factors are required. The ultimate goal is to apply the formalism to simulate multihadron systems in lattice QCD. There, the hadron states emerge from dynamics based on quark and gluon degrees of freedom. Hence the noninteracting two-particle correlation function depends on extra renormalization factors. How the renormalization should be dealt with in real lattice QCD simulations is not clear at this stage and requires further studies and developments.

ACKNOWLEDGMENTS

This research is supported by the U.S. National Science Foundation under Grant No. PHY-2418937 (P. G.) and in part Grant No. PHY-2309135 to the Kavli Institute for Theoretical Physics (KITP) (P. G.), and the U.S. Department of Energy under Grant No. DE-FG02-95ER40907 (F. L. and A. A.). Numerical simulations are carried out on Perlmutter at NERSC and local clusters at DSU and GWU.

DATA AVAILABILITY

The data are not publicly available. The data are available from the authors upon reasonable request.

APPENDIX A: RELATIVISTIC SCATTERING SOLUTIONS WITH A CONTACT INTERACTION IN INFINITE VOLUME

1. Relativistic Lippmann-Schwinger like equation and scattering solutions

For the complex ϕ^4 theory with an instantaneous and contact interaction in the form of Eq. (7), the scattering dynamics can be well-described by relativistic Lippmann-Schwinger (LS)-like equation, see e.g., Refs. [14,36]. The relativistic wave function with an incoming plane wave, $e^{i\mathbf{k}\cdot\mathbf{r}}$, satisfies

$$\psi^{(\infty)}_{E_k}(\mathbf{r},\mathbf{k}) = e^{i\mathbf{k}\cdot\mathbf{r}} + G^{(0,\infty)}(\mathbf{r},E_k)V_0\psi^{(\infty)}_{E_k}(\mathbf{0},\mathbf{k}), \quad \text{(A1)}$$

where $\mathbf{r}$ and $\mathbf{k}$ are the relative coordinate and momentum of two particles in the center-of-mass frame, and V_0 denotes the bare contact interaction strength. The total energy of two identical scalar particles with mass of m is related to momentum $\mathbf{k}$ via the relativistic dispersion relation,

$$E_k = 2\sqrt{\mathbf{k}^2+m^2}. \quad \text{(A2)}$$

The free-particle Green's function is defined by

$$G^{(0,\infty)}(\mathbf{r};E) = \int_{-\infty}^{\infty}\frac{d\mathbf{q}}{(2\pi)^3}\frac{1}{\sqrt{\mathbf{q}^2+m^2}}\frac{e^{i\mathbf{q}\cdot\mathbf{r}}}{E^2-E_q^2+i0}. \quad \text{(A3)}$$

With a contact interaction, only S-wave will contribute to nontrivial scattering solutions. By introducing the S-wave scattering amplitude,

$$t(E) = -\frac{1}{\frac{1}{V_0}-G^{(0,\infty)}(\mathbf{0};E)}, \quad \text{(A4)}$$

the scattering solution for wave function is given by

$$\psi^{(\infty)}_{E_k}(\mathbf{r},\mathbf{k}) = e^{i\mathbf{k}\cdot\mathbf{r}} - t(E_k)G^{(0,\infty)}(\mathbf{r};E_k). \quad \text{(A5)}$$

The Green's function $G^{(0,\infty)}(\mathbf{0};E)$ is an analytic function of E^2 with a branch cut starting at threshold $4m^2$,

$$G^{(0,\infty)}(\mathbf{0};E) = \frac{1}{16\pi^2}\int_{4m^2}^{\infty}ds'\frac{\sqrt{1-\frac{4m^2}{s'}}}{E^2-s'+i0}. \quad \text{(A6)}$$

The imaginary part of Green's function at $\mathbf{r}=\mathbf{0}$ is finite,

$$\mathrm{Im}\left[G^{(0,\infty)}(\mathbf{0};E)\right] = \begin{cases} -\frac{1}{16\pi}\sqrt{1-\frac{4m^2}{E^2}}, & \text{if } E>4m^2; \\ 0, & \text{otherwise.} \end{cases} \quad \text{(A7)}$$

However, the real part of Green's function at $\mathbf{r}=\mathbf{0}$ diverges logarithmically and is cutoff dependent, see Eq. (B4) in Ref. [14],

$$\mathrm{Re}[G^{(0,\infty)}(\mathbf{0};E)] = \mathrm{Re}[G(E)] - \frac{1}{8\pi^2}\ln\frac{2\Lambda}{m}, \quad \text{(A8)}$$

where Λ denotes the momentum cutoff. The function $G(E)$ in this equation is divergence-free and well-defined,

$$G(E) = \frac{\rho(E)}{\pi}\ln\frac{\rho(E)+1}{\rho(E)-1}, \quad \text{(A9)}$$

where

$$\rho(E) = \frac{1}{16\pi}\sqrt{1-\frac{4m^2}{E^2}}. \quad \text{(A10)}$$

The divergence term of Green's function in the definition of scattering amplitude can be absorbed by redefining the bare coupling strength,

$$\frac{1}{V_0} = \frac{1}{V_R(\mu)} + G(\mu) - \frac{1}{8\pi^2}\ln\frac{2\Lambda}{m}, \quad \text{(A11)}$$

where $V_R(\mu)$ is the renormalized coupling strength at a renormalization scale μ with μ chosen below two-particle threshold. Hence we find

$$t(E) = -\frac{1}{\frac{1}{V_R(\mu)} - G(E) + G(\mu)}. \quad \text{(A12)}$$

The scattering amplitude is typically parametrized by a phase shift,

$$t(E) = \frac{1}{\rho(E)}\frac{e^{2i\delta(E)}-1}{2i} = \frac{1}{\rho(E)}\frac{1}{\cot\delta(E) - i}, \quad \text{(A13)}$$

so the S-wave phase shift is given by

$$\delta(E) = \cot^{-1}\left[-\frac{\frac{1}{V_R(\mu)} - \mathrm{Re}[G(E)] + G(\mu)}{\rho(E)}\right]. \quad \text{(A14)}$$

The Muskhelishvili-Omnès (MO) representation [59–61] of scattering amplitude is associated with the phase shift via a dispersion integral relation by

$$t(E) = N e^{\frac{1}{\pi}\int_{4m^2}^{\infty} ds \frac{\delta(\sqrt{s})}{s-E^2-i0}}, \quad \text{(A15)}$$

where

$$N = t(\mu) e^{-\frac{1}{\pi}\int_{4m^2}^{\infty} ds \frac{\delta(\sqrt{s})}{s-\mu^2}}, \quad \text{(A16)}$$

is a constant normalization factor.

Using analytic expression of the scattering amplitude, we can verify that the scattering amplitude satisfies a generalized unitarity relation,

$$t(E) - t^*(E') = [G^{(0,\infty)}(\mathbf{0};E) - G^{(0,\infty)*}(\mathbf{0};E')]t^*(E')t(E). \quad \text{(A17)}$$

The ultraviolet divergence of Green's function at $\mathbf{r} = \mathbf{0}$ is cancelled out on the right-hand side of Eq. (A17), and the generalized unitarity relation is free of divergence. This relation guarantees that the scattering amplitude in Eqs. (A12) and (A13) is well-defined.

2. Two-particle Green's function solution with a contact interaction

The solution of relativistic two-particle Green's function with a contact interaction is given by Dyson equation,

$$G^{(\infty)}(\mathbf{r},\mathbf{r}';E) = G^{(0,\infty)}(\mathbf{r}-\mathbf{r}';E) + G^{(0,\infty)}(\mathbf{r};E)V_0 G^{(\infty)}(\mathbf{0},\mathbf{r}';E). \quad \text{(A18)}$$

Using Eq. (A4), it can be written in terms of $t(E)$ matrix as

$$G^{(\infty)}(\mathbf{r},\mathbf{r}';E) - G^{(0,\infty)}(\mathbf{r}-\mathbf{r}';E) = -G^{(0,\infty)}(\mathbf{r};E)t(E)G^{(0,\infty)}(\mathbf{r}';E). \quad \text{(A19)}$$

The spectral representation of Green's function is given by

$$G^{(\infty)}(\mathbf{r},\mathbf{r}';E) = \int_{-\infty}^{\infty}\frac{d\mathbf{q}}{(2\pi)^3}\frac{1}{\sqrt{\mathbf{q}^2+m^2}} \times \frac{\psi^{(\infty)}_{E_q}(\mathbf{r},\mathbf{q})\psi^{(\infty)*}_{E_q}(\mathbf{r}',\mathbf{q})}{E^2-E_q^2+i0}, \quad \text{(A20)}$$

where $E_q = 2\sqrt{\mathbf{q}^2+m^2}$.

3. Relativistic integrated Green's function and generalized Krein's theorem

Fourier transforming Eq. (A19) into momentum space, we find,

$$\sqrt{p^2+m^2}[\tilde{G}^{(\infty)}(\mathbf{p},\mathbf{p};E) - \tilde{G}^{(0,\infty)}(\mathbf{p}-\mathbf{p};E)] = t(E)\frac{d}{dE^2}\left[\frac{1}{\sqrt{p^2+m^2}}\frac{1}{E^2-E_p^2+i0}\right], \quad \text{(A21)}$$

where the Green's function in momentum space is defined by

$$\tilde{G}^{(\infty)}(\mathbf{p},\mathbf{p}';E) = \int_{-\infty}^{\infty} d\mathbf{r}d\mathbf{r}' e^{i\mathbf{p}\cdot\mathbf{r}}G^{(\infty)}(\mathbf{r},\mathbf{r}';E)e^{-i\mathbf{p}'\cdot\mathbf{r}'}. \quad \text{(A22)}$$

The difference of integrated Green's functions is therefore given by

$$\int_{-\infty}^{\infty}\frac{d\mathbf{p}}{(2\pi)^3}\sqrt{p^2+m^2}[\tilde{G}^{(\infty)}(\mathbf{p},\mathbf{p};E)-\tilde{G}^{(0,\infty)}(\mathbf{0};E)] = t(E)\frac{d}{dE^2}G^{(0,\infty)}(\mathbf{0},E) = -\frac{d}{dE^2}\ln[t(E)]. \tag{A23}$$

Using Eq. (A15), the integrated Green's function is associated with the scattering phase shift by

$$\int_{-\infty}^{\infty}\frac{d\mathbf{p}}{(2\pi)^3}\sqrt{p^2+m^2}[\tilde{G}^{(\infty)}(\mathbf{p},\mathbf{p};E)-\tilde{G}^{(0,\infty)}(\mathbf{0};E)] = -\frac{1}{\pi}\int_{4m^2}^{\infty}ds\frac{\delta(\sqrt{s})}{(s-E^2-i0)^2}, \tag{A24}$$

and we also have a relation for the imaginary part,

$$\int_{-\infty}^{\infty}\frac{d\mathbf{p}}{(2\pi)^3}\sqrt{p^2+m^2}\,\mathrm{Im}\,[\tilde{G}^{(\infty)}(\mathbf{p},\mathbf{p};E)-\tilde{G}^{(0,\infty)}(\mathbf{0};E)] = -\frac{d\delta(E)}{dE^2}. \tag{A25}$$

The relations in Eqs. (A25) and (A24) are a relativistic generalization of Friedel formula [62] and Krein's theorem [63,64] respectively, also see discussions in Ref. [61]. Using the partial-wave expansion of Green's function,

$$\tilde{G}^{(\infty)}(\mathbf{p},\mathbf{p}';E) = \sum_{lm_l}Y_{lm_l}(\hat{\mathbf{p}})\tilde{G}_l^{(\infty)}(p,p';E)Y^*_{lm_l}(\widehat{\mathbf{p}'}), \tag{A26}$$

the relation can be written in terms of partial waves,

$$\int_0^{\infty}\frac{p^2dp}{(2\pi)^3}\sqrt{p^2+m^2}[\tilde{G}_l^{(\infty)}(p,p;E)-\tilde{G}_l^{(0,\infty)}(0;E)] = -\frac{1}{\pi}\int_{4m^2}^{\infty}ds\frac{\delta_l(\sqrt{s})}{(s-E^2-i0)^2}. \tag{A27}$$

APPENDIX B: THE INTEGRATED CORRELATION FUNCTION FORMALISM FOR A COMPLEX ϕ^4 LATTICE MODEL

In this section, we present some technical details of the integrated correlation function formalism for a simple relativistic lattice model in $3+1$ spacetime dimensions. Its $1+1$ correspondence can be found in Ref. [53]. We consider the complex ϕ^4 model with interaction of charged scalar particles via a short range potential whose classical action in four-dimensional Minkowski space-time is

$$S = \frac{1}{2}\int_{-\infty}^{\infty}dt\int_0^L d\mathbf{x}\left[\frac{\partial\phi^*}{\partial t}\frac{\partial\phi}{\partial t}-\nabla\phi^*\cdot\nabla\phi-m_0^2|\phi|^2\right] - \frac{g_0}{4!}\int_{-\infty}^{\infty}dt\int_0^L d\mathbf{x}|\phi(\mathbf{x},t)|^4, \tag{B1}$$

where m_0 and g_0 are the bare mass and coupling strength of charged scalar field. The action is written down in a finite box of size L and continuous time t. The complex $\phi(\mathbf{x},t)$ field operator satisfies the periodic boundary condition,

$$\phi(\mathbf{x}+L\hat{\mathbf{x}},t) = \phi(\mathbf{x},t), \tag{B2}$$

where $\hat{\mathbf{x}}$ stands for the spatial dimensional unit vector. Its discretization in Euclidean spactime in Eq. (14) is used in Monte Carlo simulations.

1. Two-particle correlation function and its spectral representation

The two-particle interaction is encoded in the time dependence of correlation functions defined by

$$C^{(2\phi)}(\mathbf{r}t;\mathbf{r}'0) = \theta(t)\langle 0|\mathcal{O}(\mathbf{r},t)\mathcal{O}^\dagger(\mathbf{r}',0)|0\rangle + \theta(-t)\langle 0|\mathcal{O}^\dagger(\mathbf{r}',0)\mathcal{O}(\mathbf{r},t)|0\rangle, \tag{B3}$$

where $\mathcal{O}^\dagger(\mathbf{r}',0)$ and $\mathcal{O}(\mathbf{r},t)$ creates and annihilates two identical charged particles with relative coordinates and time at $(\mathbf{r}',0)$ and $(\mathbf{r},t)$, respectively. The creation operator after projecting out center-of-mass motion in the rest frame is defined by

$$\mathcal{O}^\dagger(\mathbf{r},t) = \frac{1}{\sqrt{2}}\int_0^L\frac{d\mathbf{x}_2}{\sqrt{L^3}}\phi(\mathbf{r}+\mathbf{x}_2,t)\phi(\mathbf{x}_2,t). \tag{B4}$$

The factor $1/\sqrt{2}$ takes into account the exchange symmetry of two distinguishable charged particles. Inserting a complete energy basis, $\sum_n|E_n\rangle\langle E_n| = 1$, and also defining two-particle and two-antiparticle relative wave functions,

$$\langle E_n|\mathcal{O}^\dagger(\mathbf{r}',0)|0\rangle = \frac{1}{\sqrt{L^3}}\frac{\psi^{(L)*}_{E_n}(\mathbf{r}')}{E_n}, \qquad \langle E_n|\mathcal{O}(\mathbf{r},t)|0\rangle = \frac{1}{\sqrt{L^3}}\frac{\psi^{(L)*}_{E_n}(\mathbf{r})}{E_n}e^{iE_nt}, \tag{B5}$$

where we have assumed that two-particle and two-antiparticle wave functions are identical, the spectral representation of relativistic two-particle correlation function can be written as

$$C^{(2\phi)}(\mathbf{r}t;\mathbf{r}'0) = \frac{\theta(t)}{L^3}\sum_n\frac{\psi^{(L)}_{E_n}(\mathbf{r})}{E_n}\frac{\psi^{(L)*}_{E_n}(\mathbf{r}')}{E_n}e^{-iE_nt} + \frac{\theta(-t)}{L^3}\sum_n\frac{\psi^{(L)}_{E_n}(\mathbf{r}')}{E_n}\frac{\psi^{(L)*}_{E_n}(\mathbf{r})}{E_n}e^{iE_nt}. \tag{B6}$$

In the absence of interactions, the correlation function takes the form of

$$C^{(0,2\phi)}(\mathbf{r}t;\mathbf{r}'0) = \frac{1}{L^3}\sum_{\mathbf{p}=\frac{2\pi\mathbf{n}}{L},\mathbf{n}\in\mathbb{Z}^3}\frac{\cos(\mathbf{p}\cdot\mathbf{r})}{E_p^{(0)}}\frac{\cos(\mathbf{p}\cdot\mathbf{r}')}{E_p^{(0)}}e^{-iE_p^{(0)}|t|}, \quad \text{(B7)}$$

where free two-particle energies are $E_p^{(0)} = 2\sqrt{\mathbf{p}^2+m^2}$ with $\mathbf{p} = \frac{2\pi\mathbf{n}}{L}, \mathbf{n}\in\mathbb{Z}^3$.

The two-particle relative wave function satisfies relativistic LS-like equation, see e.g., Appendix A,

$$\psi_E^{(L)}(\mathbf{r}) = V_0 G^{(0,L)}(\mathbf{r};E)\psi_E^{(L)}(\mathbf{0}). \quad \text{(B8)}$$

The relativistic finite volume Green's function is defined by, see e.g., Refs. [14,36],

$$G^{(0,L)}(\mathbf{r};E) = \frac{1}{L^3}\sum_{\mathbf{q}=\frac{2\pi\mathbf{n}}{L},\mathbf{n}\in\mathbb{Z}^3}\frac{1}{\omega_q}\frac{e^{i\mathbf{q}\cdot\mathbf{r}}}{E^2-(2\omega_q)^2}, \quad \text{(B9)}$$

where $\omega_q = \sqrt{\mathbf{q}^2+m^2}$ is the energy of a single particle with momentum $\mathbf{q}$. The two-particle wave function must be symmetric due to Bose symmetry,

$$\psi_{E_n}^{(L)}(-\mathbf{r}) = \psi_{E_n}^{(L)}(\mathbf{r}). \quad \text{(B10)}$$

The relativistic wave function is normalized in momentum space by

$$\frac{1}{L^3}\sum_{\mathbf{p}=\frac{2\pi\mathbf{n}}{L},\mathbf{n}\in\mathbb{Z}^3}\frac{1}{2\omega_p}\tilde{\psi}_{E_n}^{(L)}(\mathbf{p})\tilde{\psi}_{E_{n'}}^{(L)*}(\mathbf{p}) = E_n L^3\frac{\delta_{n,n'}+\delta_{n,-n'}}{2}, \quad \text{(B11)}$$

where the Fourier transform of wave function is defined by

$$\frac{\tilde{\psi}_{E_n}^{(L)}(\mathbf{p})}{2\omega_p} = \int_0^L d\mathbf{r}\psi_{E_n}^{(L)}(\mathbf{r})e^{i\mathbf{p}\cdot\mathbf{r}}. \quad \text{(B12)}$$

The normalization relation of wave function in Eq. (B11) leads to cubic symmetry A_1^+ irrep projected integrated correlation function,

$$C_{A_1^+}^{(2\phi)}(t) = \frac{1}{L^3}\sum_{\mathbf{p}=\frac{2\pi\mathbf{n}}{L},\mathbf{n}\in\mathbb{Z}^3}2\omega_p\tilde{C}_{A_1^+}^{(2\phi)}(\mathbf{p}t;\mathbf{p}0) = \sum_n\frac{e^{-iE_n|t|}}{E_n}, \quad \text{(B13)}$$

where $\tilde{C}_{A_1^+}^{(2\phi)}$ is the integrated correlation function in momentum space. Its Fourier transform and A_1^+ irrep projection are performed by

$$\tilde{C}^{(2\phi)}(\mathbf{p}t;\mathbf{p}'0) = \int_0^L d\mathbf{r}d\mathbf{r}'e^{i\mathbf{p}\cdot\mathbf{r}}C^{(2\phi)}(\mathbf{r}t;\mathbf{r}'0)e^{-i\mathbf{p}'\cdot\mathbf{r}'} \quad \text{(B14)}$$

and

$$\tilde{C}_{A_1^+}^{(2\phi)}(\mathbf{p}t;\mathbf{p}'0) = \frac{1}{48^2}\sum_{(g,g')\in\mathcal{G}}\tilde{C}^{(2\phi)}(g\mathbf{p}t;g'\mathbf{p}'0). \quad \text{(B15)}$$

The $(\mathcal{G},g)$ stand for the cubic symmetry octahedral group O_h and its elements, see e.g., Refs. [14,28,58]. We remark that only A_1^+ irrep is projected in this work since the ϕ^4 theory is equivalent to a contact interaction theory, hence only S-wave contributes to the scattering dynamics.

Using the relation,

$$\left|\frac{1}{48}\sum\nolimits_{g\in\mathcal{G}}\left[\int d\mathbf{r}e^{ig\mathbf{p}_0\cdot\mathbf{r}}\cos(\mathbf{k}\cdot\mathbf{r})\right]\right|^2 = \begin{cases}\frac{L^6}{\vartheta^2(\mathbf{p}_0)}, & \text{if } \mathbf{k}\in g\mathbf{p}_0, \text{where } g\in\mathcal{G},\\ 0, & \text{otherwise,}\end{cases} \quad \text{(B16)}$$

where $\mathbf{p}_0$ denote a single reference vector, the set of momenta represented by $\mathbf{p}_0$ via $\mathbf{p} = g\mathbf{p}_0(g\in\mathcal{G})$ is called the "star" of $\mathbf{p}_0$, and $\vartheta(\mathbf{p}_0)$ is the multiplicity of distinct momenta within the set represented by $\mathbf{p}_0$, see e.g., Refs. [14,28,58], we can thus show that

$$C_{A_1^+}^{(0,2\phi)}(t) = \sum_{\mathbf{p}_0}\frac{e^{-iE_{\mathbf{p}_0}^{(0)}|t|}}{E_{\mathbf{p}_0}^{(0)}}. \quad \text{(B17)}$$

The reference vectors, $\mathbf{p}_0$'s, may be chosen as

$$\mathbf{p}_0 = \frac{2\pi}{L}(i,j,k), \quad (i,j,k)\in[0,1,\ldots]\,\&\,(i\le j\le k). \quad \text{(B18)}$$

The sum of momenta over a general function can be reorganized as follows:

$$\sum_{\mathbf{p}=\frac{2\pi\mathbf{n}}{L},\mathbf{n}\in\mathbb{Z}^3}f(\mathbf{p}) = \sum_{\mathbf{p}_0}\vartheta(\mathbf{p}_0)\frac{1}{48}\sum_{g\in\mathcal{G}}f(g\mathbf{p}_0). \quad \text{(B19)}$$

Hence instead of using label n, we can use $\mathbf{p}_0$ to label all the eigenenergies; $n\to\mathbf{p}_0$ and $E_n\to E_{\mathbf{p}_0}$. We thus should also have a similar relation as in Eq. (B17) for interacting wave function,

$$\left|\frac{1}{48}\sum\nolimits_{g\in\mathcal{G}}\left[\int d\mathbf{r}e^{ig\mathbf{p}_0\cdot\mathbf{r}}\psi_{E_{\mathbf{k}}}^{(L)}(\mathbf{r})\right]\right|^2 = \begin{cases}\frac{L^6}{\vartheta^2(\mathbf{p}_0)}, & \text{if } \mathbf{k}\in g\mathbf{p}_0, \text{where } g\in\mathcal{G},\\ 0, & \text{otherwise.}\end{cases} \quad \text{(B20)}$$

The spectral representation of difference of interacting and noninteracting integrated correlation functions in A_1^+ irrep is thus given by

$$\begin{aligned}&\triangle C^{(2\phi)}_{A_1^+}(t)\\&=\frac{1}{L^3}\sum_{\mathbf{p}=\frac{2\pi\mathbf{n}}{L},\mathbf{n}\in\mathbb{Z}^3}2\omega_p\left[\tilde{C}_{A_1^+}(\mathbf{p}t;\mathbf{p}0)-\tilde{C}^{(0)}_{A_1^+}(\mathbf{p}t;\mathbf{p}0)\right]\\&=\sum_{\mathbf{p}_0}\left[\frac{e^{-iE_{\mathbf{p}_0}t}}{E_{\mathbf{p}_0}}-\frac{e^{-iE^{(0)}_{\mathbf{p}_0}t}}{E^{(0)}_{\mathbf{p}_0}}\right].\end{aligned}\tag{B21}$$

Therefore, there are two ways to obtain the difference of integrated correlations in the main relation in Eq. (13), either by direct calculation plus Fourier transform, or by energy spectrum if it is available.

2. Relating integrated correlation functions to scattering phase shift

Conisder the momentum-space spectral representation of two-particle correlation function along the diagonal,

$$\begin{aligned}&\tilde{C}^{(2\phi)}(\mathbf{p}t;\mathbf{p}0)\\&=\frac{1}{L^3}\sum_n\frac{1}{E_n^2}\frac{|\tilde{\psi}^{(L)}_{E_n}(\mathbf{p})|^2}{E_p^2}[\theta(t)e^{-iE_nt}+\theta(-t)e^{iE_nt}].\end{aligned}\tag{B22}$$

Using the identity,

$$i\int_{-\infty}^{\infty}\frac{d\lambda}{2\pi}\frac{e^{-i\lambda t}}{\lambda+i0}=\theta(t),\tag{B23}$$

the diagonal element of two-particle correlation function can be related to two-particle Green's function by

$$\tilde{C}^{(2\phi)}(\mathbf{p}t;\mathbf{p}0)=i\int_{-\infty}^{\infty}\frac{d\lambda}{2\pi}\tilde{G}^{(L)}(\mathbf{p},\mathbf{p};\lambda)e^{-i\lambda t}.\tag{B24}$$

The spectral representation of two-particle Green's function in finite volume is given by

$$G^{(L)}(\mathbf{r},\mathbf{r}';E)=\frac{1}{L^3}\sum_{\mathbf{q}=\frac{2\pi\mathbf{n}}{L},\mathbf{n}\in\mathbb{Z}^3}\frac{1}{\omega_q}\frac{\psi^{(L)}_{E_q}(\mathbf{r})\psi^{(L)*}_{E_q}(\mathbf{r}')}{E^2-E_q^2+i0},\tag{B25}$$

and $E_q=2\omega_q=2\sqrt{q^2+m^2}$. It is the lattice version of Eq. (A20). The momentum space two-particle Green's function, $\tilde{G}^{(L)}(\mathbf{p},\mathbf{p}';E)$, is the Fourier transform of coordinate space two-particle Green's function,

$$\tilde{G}^{(L)}(\mathbf{p},\mathbf{p}';E)=\int_0^L d\mathbf{r}d\mathbf{r}'e^{i\mathbf{p}\cdot\mathbf{r}}G^{(L)}(\mathbf{r},\mathbf{r}';E)e^{-i\mathbf{p}'\cdot\mathbf{r}'},\tag{B26}$$

which is lattice version of Eq. (A21). The difference of integrated correlation functions in A_1^+ irrep is related to finite volume Green's functions by

$$\begin{aligned}\triangle C^{(2\phi)}_{A_1^+}(t)=i\int_{-\infty}^{\infty}\frac{d\lambda}{2\pi}e^{-i\lambda t}\\\times\frac{1}{L^3}\sum_{\mathbf{p}=\frac{2\pi\mathbf{n}}{L},\mathbf{n}\in\mathbb{Z}^3}2\omega_p\left[\tilde{G}^{(L)}_{A_1^+}(\mathbf{p},\mathbf{p};\lambda)-\tilde{G}^{(0,L)}_{A_1^+}(\mathbf{0};\lambda)\right].\end{aligned}\tag{B27}$$

The A_1^+ irrep projected Green's functions are defined by

$$\tilde{G}^{(L)}_{A_1^+}(\mathbf{p},\mathbf{p}';\lambda)=\frac{1}{48^2}\sum_{(g,g')\in\mathcal{G}}\tilde{G}^{(L)}(g\mathbf{p},g'\mathbf{p}';\lambda).\tag{B28}$$

Using relativistic Friedel formula and Krein's theorem relations in infinite volume, see Appendix A 3,

$$\begin{aligned}&\int_{-\infty}^{\infty}\frac{d\mathbf{p}}{(2\pi)^3}\omega_p[\tilde{G}^{(\infty)}(\mathbf{p},\mathbf{p};E)-\tilde{G}^{(0,\infty)}(\mathbf{0};E)]\\&=-\frac{1}{\pi}\int_{4m^2}^{\infty}ds\frac{\delta(\sqrt{s})}{(s-E^2-i0)^2},\end{aligned}\tag{B29}$$

where $\delta(E)$ is the S-wave scattering phase shift of two scalar particles, the difference of integrated correlation functions thus approaches its infinite volume limit by

$$\triangle C^{(2\phi)}_{A_1^+}(t)\overset{L\to\infty}{\to}-\frac{1}{\pi}\int_{4m^2}^{\infty}ds\delta(\sqrt{s})\left[i\int_{-\infty}^{\infty}\frac{d\lambda}{\pi}\frac{e^{-i\lambda t}}{(s-\lambda^2-i0)^2}\right].\tag{B30}$$

Completing the integration in the bracket, we find a compact relation in Eq. (12) that closely resembles its $1+1$ dimensional counterpart in Ref. [53].

3. Quantization condition in finite volume

With a contact interaction defined in Eq. (7), the quantization condition can be obtained via Eq. (B8),

$$\frac{1}{V_0}=G^{(0,L)}(\mathbf{0};E),\tag{B31}$$

where the finite volume free two-particle Green's function is given in Eq. (B9). Using Eqs. (A4) and (A13), the potential strength V_0 can be related to infinite volume free particles Green's function and scattering phase shift by

$$\frac{1}{V_0}=\mathrm{Re}[G^{(0,\infty)}(\mathbf{0};E)]-\rho(E)\cos\delta(E),\tag{B32}$$

where the analytic expression of $G^{(0,\infty)}(0;E)$ and $\rho(E)$ are given in Eqs. (A3) and (A10), respectively. The quantization condition can be rewritten in a compact form known as Lüscher formula,

$$\cos\delta(E) = \frac{\mathrm{Re}[G^{(0,\infty)}(\mathbf{0};E)] - G^{(0,L)}(\mathbf{0};E)}{\rho(E)}, \tag{B33}$$

the right-hand side of Eq. (B33) is typically referred to zeta function, see e.g., Ref. [1]. The above discussion demonstrates the indirect connection via Green's functions between the ICF formalism and the Lüscher formalism.

4. Perturbation result

The perturbation calculation of integrated correlation functions in a periodic box of size L can be carried out in a similar fashion as in Ref. [53,54]. The leading-order contribution of the difference of integrated correlation functions in finite volume is given by

$$\begin{aligned} &C^{(2\phi)}(\mathbf{r},t;\mathbf{r}',0) - C^{(0,2\phi)}(\mathbf{r},t;\mathbf{r}',0) \\ &\simeq -\frac{iV_R(0)}{L^3}\int_0^L d\mathbf{x}_2 \int_0^L d\mathbf{x}'_2 \int_{-\infty}^{\infty} dt' \int_0^L d\mathbf{x}'' \\ &\quad \times D_0^{-1}(\mathbf{r}+\mathbf{x}_2-\mathbf{x}'', t-t'') D_0^{-1}(\mathbf{x}_2-\mathbf{x}'', t-t'') \\ &\quad \times D_0^{-1}(\mathbf{x}''-\mathbf{r}'-\mathbf{x}'_2, t'') D_0^{-1}(\mathbf{x}''-\mathbf{x}'_2, t''), \end{aligned} \tag{B34}$$

where $V_R(0)$ is the renormalized contact potential strength with renormalization scale chosen at $\mu = 0$, and D_0^{-1} the free two-particle propagator defined by

$$D_0^{-1}(\mathbf{x},t) = i\int_{-\infty}^{\infty}\frac{d\epsilon}{2\pi}\frac{1}{L^3}\sum_{\mathbf{k}=\frac{2\pi\mathbf{n}}{L},\mathbf{n}\in\mathbb{Z}^3}\frac{e^{ikx}e^{i\epsilon t}}{\epsilon^2-(k^2+m^2)}. \tag{B35}$$

After carrying out the space and time integrations, we find

$$\begin{aligned} &C^{(2\pi)}(\mathbf{r},t;\mathbf{r}',0) - C^{(0,2\phi)}(\mathbf{r},t;\mathbf{r}',0) \\ &\quad \simeq -iV_R(0)\int_{-\infty}^{\infty}\frac{d\epsilon}{2\pi}e^{i\epsilon t}G^{(0,L)}(\mathbf{r};\epsilon)G^{(0,L)}(\mathbf{r}';\epsilon), \end{aligned} \tag{B36}$$

in terms of the finite volume free-particle Green's function defined in Eq. (B9). Using the spectral representation in Eq. (B21) and carrying out the integration of ϵ, we obtain the leading-order result from perturbation theory,

$$\triangle C^{(2\phi)}_{\mathrm{pert}}(t) \simeq -\frac{V_R(0)}{L^3}\sum_{\mathbf{k}=\frac{2\pi\mathbf{n}}{L},\mathbf{n}\in\mathbb{Z}^3}\frac{it+\frac{1}{E_k}}{E_k^3}e^{-iE_kt}, \tag{B37}$$

where $E_k = 2\sqrt{k^2+m^2}$. It approaches the infinite volume limit by

$$\triangle C^{(2\phi)}_{\mathrm{pert}}(t) \overset{L\to\infty}{\to} -V_R(0)\int_{-\infty}^{\infty}\frac{d\mathbf{k}}{(2\pi)^3}\frac{it+\frac{1}{E_k}}{E_k^3}e^{-iE_kt}. \tag{B38}$$

On the other hand, using the perturbation expansion of scattering phase shift via Eqs. (B32) and (A10),

$$\delta(E_k) \simeq -V_R(0)\rho(E_k) = -\frac{V_R(0)}{16\pi}\frac{2k}{E_k}, \tag{B39}$$

we can verify that,

$$\begin{aligned} &-\frac{1}{\pi}\int_{2m}^{\infty}d\epsilon\delta(\epsilon)\frac{d}{d\epsilon}\left(\frac{e^{-it\epsilon t}}{\epsilon}\right) \\ &\quad \simeq -V_R(0)\int_{-\infty}^{\infty}\frac{d\mathbf{k}}{(2\pi)^3}\left(it+\frac{1}{E_k}\right)\frac{e^{-iE_kt}}{E_k^3}, \end{aligned} \tag{B40}$$

which is Eq. (B38).

On the finite Euclidean spacetime lattice $L^3\times T$, the perturbation result for the difference of integrated correlation function takes the form,

$$\triangle C^{(2\phi)}_{\mathrm{pert}}(\tau) = \frac{1}{L^3}\sum_{\mathbf{p}=\frac{2\pi\mathbf{n}}{L}}^{\mathbf{n}\in[-\frac{L}{2}+1,\frac{L}{2}]^3} 2\omega^{(\mathrm{lat})}_{\mathbf{p}}\triangle\tilde{C}^{(2\phi)}_{\mathrm{pert}}(\mathbf{p},\tau), \tag{B41}$$

where the momentum-space result before integration is

$$\triangle\tilde{C}^{(2\phi)}_{\mathrm{pert}}(\mathbf{p},\tau) = -\frac{V_R(0)}{T}\sum_{\omega=\frac{2\pi n}{L}}^{n\in[0,T-1]} e^{i\omega\tau}[G_{2\phi}(\mathbf{p},\omega)]^2. \tag{B42}$$

The finite volume two-particle Green's function is defined by

$$\begin{aligned} &G_{2\phi}(\mathbf{p},\omega) \\ &= \frac{1}{T}\sum_{\omega'=\frac{2\pi n'}{L}}^{n'\in[0,T-1]}\frac{1}{\sum_i(2-2\cos\mathbf{k}_i)-2\cos\omega'+2\cosh m} \\ &\quad \times\frac{1}{\sum_i(2-2\cos\mathbf{k}_i)-2\cos(\omega-\omega')+2\cosh m}. \end{aligned} \tag{B43}$$

In the limit of $T\to\infty$ and zero lattice spacing, it takes the simple form,

$$G_{2\phi}(p,\omega) \overset{T\to\infty}{\underset{a\to0}{\to}} \frac{1}{\omega_p}\frac{1}{\omega^2+(2\omega_p)^2}, \tag{B44}$$

which leads to the difference of two-particle correlation functions,

$$\triangle\tilde{C}^{(2\phi)}_{\mathrm{pert}}(\mathbf{p},\tau) \overset{T\to\infty}{\underset{a\to0}{\to}} -V_R(0)\frac{\tau+\frac{1}{2\omega_p}}{(2\omega_p)^4}e^{-2\omega_p\tau}, \tag{B45}$$

and its integrated version,

$$\triangle C^{(2\phi)}_{\mathrm{pert}}(\tau) \overset{T\to\infty}{\underset{a\to0}{\to}} -\frac{V_R(0)}{L^3}\sum_{\mathbf{p}=\frac{2\pi\mathbf{n}}{L}}^{\mathbf{n}\in\mathbb{Z}^3}\frac{\tau+\frac{1}{2\omega_{\mathbf{p}}}}{(2\omega_{\mathbf{p}})^3}e^{-2\omega_{\mathbf{p}}\tau}. \tag{B46}$$

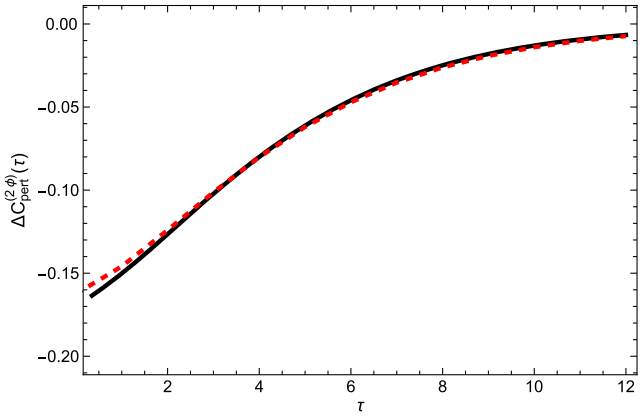


FIG. 13. Numerical check of the spectral representation in Eq. (B50); left-hand side (solid black) vs. right-hand side (dashed red). The parameters are $L = 8$, $m = 0.2$, and $V_R^{(L)}(0) = 2$.

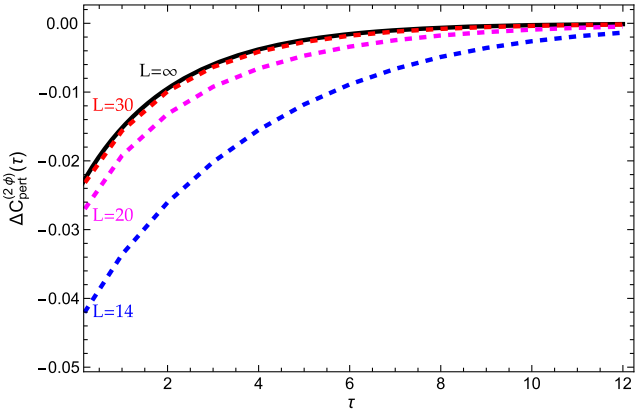


FIG. 14. Perturbation result on the right-hand side of Eq. (B50) for $L = 14$ (dashed blue), $L = 20$ (dashed magenta), and $L = 30$ (dashed red) vs. infinite volume limit of $\triangle C^{(2\phi)}(t)$ (solid black). The other parameters are $m = 0.2$ and $V_R^{(L)}(0) = 2$.

Hence, the perturbation result at the limit of zero lattice spacing in Eq. (B37) is recovered after analytic continuation $\tau \to it$.

5. Numerics

As a short summary for this appendix, the difference of integrated correlation functions in finite volume can be calculated by the spectral representation in Eq. (B21) and is related to phase shift through a weighted integral,

$$\triangle C^{(2\phi)}_{A_1^+}(t) \overset{t=-i\tau}{=} \sum_{\mathbf{p}_0} \left[\frac{e^{-E_{\mathbf{p}_0}\tau}}{E_{\mathbf{p}_0}} - \frac{e^{-2\omega_{\mathbf{p}_0}\tau}}{2\omega_{\mathbf{p}_0}}\right] \overset{L\to\infty}{\underset{t=-i\tau}{\to}} \frac{1}{\pi}\int_{2m}^{\infty} d\epsilon \delta(\epsilon)\left(\tau + \frac{1}{\epsilon}\right)\frac{e^{-\epsilon\tau}}{\epsilon}, \tag{B47}$$

where the eigenenergies $E_{\mathbf{p}_0}$ are solutions of Lüscher formula in Eq. (B33). For the contact interaction potential, instead of using Eq. (B33), we will simply introduce a finite volume dependent renormalized coupling strength by

$$\frac{1}{V_0} = \frac{1}{V_R^{(L)}(0)} + G^{(0,L)}(\mathbf{0};0), \tag{B48}$$

the renormalized quantization condition is thus given by

$$\frac{1}{V_R^{(L)}(0)} = G^{(0,L)}(\mathbf{0};E) - G^{(0,L)}(\mathbf{0};0). \tag{B49}$$

In Fig. 13, we show that the spectral representation of finite volume $\triangle C^{(2\phi)}_{A_1^+}(t)$ matches well with perturbation result:

$$\sum_{\mathbf{p}_0}\left[\frac{e^{-E_{\mathbf{p}_0}\tau}}{E_{\mathbf{p}_0}} - \frac{e^{-2\omega_{\mathbf{p}_0}\tau}}{2\omega_{\mathbf{p}_0}}\right] \overset{V_R^{(L)}(0)\sim 0}{\to} -\frac{V_R^{(L)}(0)}{L^3}\sum_{\mathbf{k}=\frac{2\pi\mathbf{n}}{L}}^{\mathbf{n}\in\mathbb{Z}^3}\frac{\tau + \frac{1}{2\omega_{\mathbf{k}}}}{(2\omega_{\mathbf{k}})^3}e^{-2\omega_{\mathbf{k}}\tau}. \tag{B50}$$

The perturbation calculation result of $\triangle C^{(2\phi)}(t)$ given by Eq. (B37) vs. its infinite volume limit is demonstrated in Fig. 14.

[1] M. Lüscher, Two particle states on a torus and their relation to the scattering matrix, Nucl. Phys. **B354**, 531 (1991).

[2] S. Aoki *et al.* (*CP*-PACS Collaboration), Lattice QCD calculation of the rho meson decay width, Phys. Rev. D **76**, 094506 (2007).

[3] X. Feng, K. Jansen, and D. B. Renner, Resonance parameters of the rho-meson from lattice QCD, Phys. Rev. D **83**, 094505 (2011).

[4] C. B. Lang, D. Mohler, S. Prelovsek, and M. Vidmar, Coupled channel analysis of the ρ meson decay in lattice QCD, Phys. Rev. D **84**, 054503 (2011); **89**, 059903(E) (2014).

[5] S. Aoki *et al.* (CS Collaboration), ρ meson decay in $2+1$ flavor lattice QCD, Phys. Rev. D **84**, 094505 (2011).

[6] J. J. Dudek, R. G. Edwards, and C. E. Thomas, S and D-wave phase shifts in isospin-$2\pi\pi$ scattering from lattice QCD, Phys. Rev. D **86**, 034031 (2012).

[7] J. J. Dudek, R. G. Edwards, and C. E. Thomas (Hadron Spectrum Collaboration), Energy dependence of the ρ resonance in $\pi\pi$ elastic scattering from lattice QCD, Phys. Rev. D **87**, 034505 (2013); **90**, 099902(E) (2014).

[8] D. J. Wilson, J. J. Dudek, R. G. Edwards, and C. E. Thomas, Resonances in coupled $\pi K, \eta K$ scattering from lattice QCD, Phys. Rev. D **91**, 054008 (2015).

[9] D. J. Wilson, R. A. Briceño, J. J. Dudek, R. G. Edwards, and C. E. Thomas, Coupled $\pi\pi, K\overline{K}$ scattering in P-wave and the ρ resonance from lattice QCD, Phys. Rev. D **92**, 094502 (2015).

[10] J. J. Dudek, R. G. Edwards, and D. J. Wilson (Hadron Spectrum Collaboration), An a_0 resonance in strongly coupled $\pi\eta$, $K\bar{K}$ scattering from lattice QCD, Phys. Rev. D **93**, 094506 (2016).

[11] S. R. Beane, W. Detmold, T. C. Luu, K. Orginos, M. J. Savage, and A. Torok, Multi-pion systems in lattice QCD and the three-pion interaction, Phys. Rev. Lett. **100**, 082004 (2008).

[12] W. Detmold, M. J. Savage, A. Torok, S. R. Beane, T. C. Luu, K. Orginos, and A. Parreno, Multi-pion states in lattice QCD and the charged-pion condensate, Phys. Rev. D **78**, 014507 (2008).

[13] B. Hörz and A. Hanlon, Two- and three-pion finite-volume spectra at maximal isospin from lattice QCD, Phys. Rev. Lett. **123**, 142002 (2019).

[14] P. Guo and B. Long, Multi-π^+ systems in a finite volume, Phys. Rev. D **101**, 094510 (2020).

[15] K. Rummukainen and S. A. Gottlieb, Resonance scattering phase shifts on a nonrest frame lattice, Nucl. Phys. **B450**, 397 (1995).

[16] N. H. Christ, C. Kim, and T. Yamazaki, Finite volume corrections to the two-particle decay of states with non-zero momentum, Phys. Rev. D **72**, 114506 (2005).

[17] V. Bernard, M. Lage, U.-G. Meißner, and A. Rusetsky, Resonance properties from the finite-volume energy spectrum, J. High Energy Phys. 08 (2008) 024.

[18] S. He, X. Feng, and C. Liu, Two particle states and the S-matrix elements in multi-channel scattering, J. High Energy Phys. 07 (2005) 011.

[19] M. Lage, U.-G. Meißner, and A. Rusetsky, A method to measure the antikaon-nucleon scattering length in lattice QCD, Phys. Lett. B **681**, 439 (2009).

[20] M. Döring, U.-G. Meißner, E. Oset, and A. Rusetsky, Unitarized chiral perturbation theory in a finite volume: Scalar meson sector, Eur. Phys. J. A **47**, 139 (2011).

[21] P. Guo, J. Dudek, R. Edwards, and A. P. Szczepaniak, Coupled-channel scattering on a torus, Phys. Rev. D **88**, 014501 (2013).

[22] P. Guo, Coupled-channel scattering in $1+1$ dimensional lattice model, Phys. Rev. D **88**, 014507 (2013).

[23] S. Kreuzer and H. W. Hammer, Efimov physics in a finite volume, Phys. Lett. B **673**, 260 (2009).

[24] K. Polejaeva and A. Rusetsky, Three particles in a finite volume, Eur. Phys. J. A **48**, 67 (2012).

[25] M. T. Hansen and S. R. Sharpe, Relativistic, model-independent, three-particle quantization condition, Phys. Rev. D **90**, 116003 (2014).

[26] M. Mai and M. Döring, Three-body unitarity in the finite volume, Eur. Phys. J. A **53**, 240 (2017).

[27] M. Mai and M. Döring, Finite-Volume Spectrum of $\pi^+\pi^+$ and $\pi^+\pi^+\pi^+$ Systems, Phys. Rev. Lett. **122**, 062503 (2019).

[28] M. Döring, H. W. Hammer, M. Mai, J. Y. Pang, A. Rusetsky, and J. Wu, Three-body spectrum in a finite volume: The role of cubic symmetry, Phys. Rev. D **97**, 114508 (2018).

[29] P. Guo, One spatial dimensional finite volume three-body interaction for a short-range potential, Phys. Rev. D **95**, 054508 (2017).

[30] P. Guo and V. Gasparian, An solvable three-body model in finite volume, Phys. Lett. B **774**, 441 (2017).

[31] P. Guo and V. Gasparian, Numerical approach for finite volume three-body interaction, Phys. Rev. D **97**, 014504 (2018).

[32] P. Guo and T. Morris, Multiple-particle interaction in $(1+1)$-dimensional lattice model, Phys. Rev. D **99**, 014501 (2019).

[33] M. Mai, M. Döring, C. Culver, and A. Alexandru, Three-body unitarity versus finite-volume $\pi^+\pi^+\pi^+$ spectrum from lattice QCD, Phys. Rev. D **101**, 054510 (2020).

[34] P. Guo, M. Döring, and A. P. Szczepaniak, Variational approach to N-body interactions in finite volume, Phys. Rev. D **98**, 094502 (2018).

[35] P. Guo, Propagation of particles on a torus, Phys. Lett. B **804**, 135370 (2020).

[36] P. Guo and M. Döring, Lattice model of heavy-light three-body system, Phys. Rev. D **101**, 034501 (2020).

[37] P. Guo, Threshold expansion formula of N bosons in a finite volume from a variational approach, Phys. Rev. D **101**, 054512 (2020).

[38] P. Guo, Myth of scattering in finite volume, arXiv:2007.04473.

[39] P. Guo and B. Long, Visualizing resonances in finite volume, Phys. Rev. D **102**, 074508 (2020).

[40] P. Guo, Modeling few-body resonances in finite volume, Phys. Rev. D **102**, 054514 (2020).

[41] P. Guo and V. Gasparian, Charged particles interaction in both a finite volume and a uniform magnetic field, Phys. Rev. D **103**, 094520 (2021).

[42] P. Guo and B. Long, Nuclear reactions in artificial traps, J. Phys. G **49**, 055104 (2022).

[43] P. Guo, Coulomb corrections to two-particle interactions in artificial traps, Phys. Rev. C **103**, 064611 (2021).

[44] P. Guo and V. Gasparian, Charged particles interaction in both a finite volume and a uniform magnetic field II: Topological and analytic properties of a magnetic system, J. Phys. A **55**, 265201 (2022).

[45] G. P. Lepage, The analysis of algorithms for lattice field theory, Boulder ASI **1989**, 97 (1989).

[46] C. Drischler, W. Haxton, K. McElvain, E. Mereghetti, A. Nicholson, P. Vranas, and A. Walker-Loud, Towards grounding nuclear physics in QCD, Prog. Part. Nucl. Phys. **121**, 103888 (2021).

[47] J. Bulava and M. T. Hansen, Scattering amplitudes from finite-volume spectral functions, Phys. Rev. D **100**, 034521 (2019).

[48] N. Ishii, S. Aoki, and T. Hatsuda, Nuclear force from lattice QCD, Phys. Rev. Lett. **99**, 022001 (2007).

[49] S. Aoki, T. Hatsuda, and N. Ishii, Theoretical foundation of the nuclear force in QCD and its applications to central and tensor forces in quenched lattice QCD simulations, Prog. Theor. Phys. **123**, 89 (2010).

[50] T. Iritani, S. Aoki, T. Doi, S. Gongyo, T. Hatsuda, Y. Ikeda, T. Inoue, N. Ishii, H. Nemura, and K. Sasaki (HAL QCD Collaboration), Systematics of the HAL QCD potential at low energies in lattice QCD, Phys. Rev. D **99**, 014514 (2019).

[51] N. Ishii, S. Aoki, T. Doi, T. Hatsuda, Y. Ikeda, T. Inoue, K. Murano, H. Nemura, and K. Sasaki, Hadron–hadron interactions from imaginary-time Nambu–Bethe–Salpeter wave function on the lattice, Phys. Lett. B **712**, 437 (2012).

[52] S. Aoki, Nucleon-nucleon interactions via lattice QCD: Methodology, Eur. Phys. J. A **49**, 81 (2013).

[53] P. Guo, Toward extracting the scattering phase shift from integrated correlation functions. II. A relativistic lattice field theory model, Phys. Rev. D **110**, 014504 (2024).

[54] P. Guo and V. Gasparian, Toward extracting the scattering phase shift from integrated correlation functions, Phys. Rev. D **108**, 074504 (2023).

[55] P. Guo and F. X. Lee, Toward extracting scattering phase shift from integrated correlation functions. III. Coupled channels, Phys. Rev. D **111**, 054506 (2025).

[56] P. Guo and F. X. Lee, Toward extracting scattering phase shifts from integrated correlation functions. IV. Coulomb corrections, Phys. Rev. D **112**, 014513 (2025).

[57] P. Guo, Toward extracting scattering phase shift from integrated correlation functions on quantum computers, arXiv:2504.14474.

[58] J. F. Cornwell, *Group Theory in Physics: An Introduction* (Academic Press, San Diego, California, 1997).

[59] N. Muskhelishvili, Application of integrals of the Cauchy type to one class of singular integral equations, Trans. Tbil. Mat. Inst. **10**, 1 (1941).

[60] R. Omnes, On the solution of certain singular integral equations of quantum field theory, Nuovo Cimento **8**, 316 (1958).

[61] P. Guo and V. Gasparian, Friedel formula and Krein's theorem in complex potential scattering theory, Phys. Rev. Res. **4**, 023083 (2022).

[62] J. Friedel, Metallic alloys, Il Nuovo Cimento (1955–1965) **7**, 287 (1958).

[63] M. S. Birman and M. Krein, On the theory of wave operators and scattering operators, Dokl. Akad. Nauk SSSR **144**, 475 (1962), https://www.mathnet.ru/php/archive.phtml?wshow=paper&jrnid=dan&paperid=26522&option_lang=eng.

[64] M. G. Krein, On the trace formula in perturbation theory, Mat. Sb. **33**, 597 (1953), https://www.mathnet.ru/php/archive.phtml?wshow=paper&jrnid=sm&paperid=5397&option_lang=eng.